

Dispersive evaluation of the two-pion channel of HVP

Thomas Leplumey

Laboratoire Leprince Ringuet — Ecole Polytechnique

in collaboration with **Peter Stoffer**

Based on the **Colangelo-Hoferichter-Kubis-Leplumey-Stoffer** (CHKLS) framework

8th plenary workshop of the muon $g - 2$ theory initiative

IJCLab, Orsay, September 9, 2024

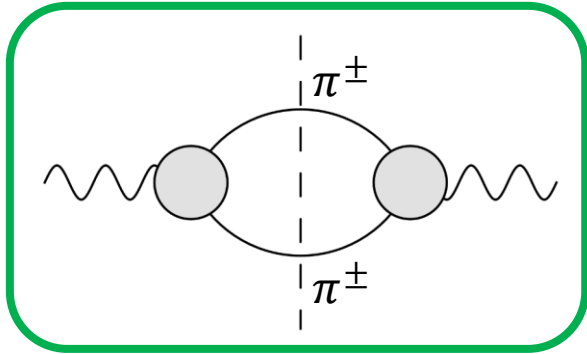


University of
Zurich^{UZH}

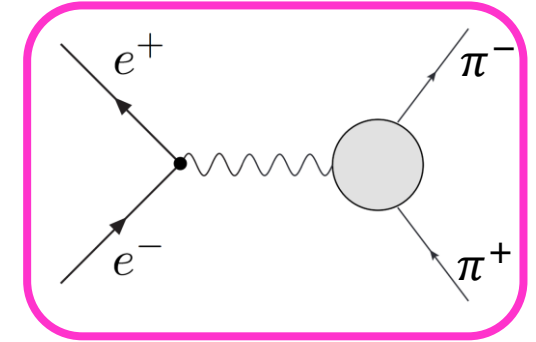


1. INTRODUCTION
2. MODEL-INDEPENDENT DESCRIPTION OF THE PION VFF
3. PARAMETERIZATION OF THE INELASTICITIES
4. METHODOLOGY FOR PARAMETER INFERENCE
5. RESULTS FOR THE 2-PION CONTRIBUTIONS TO THE HVP
6. RESULTS FOR OTHER OBSERVABLES AND CORRELATIONS WITH $a_{\mu}^{\pi\pi}$
7. CONCLUSION AND FUTURE PROSPECTS

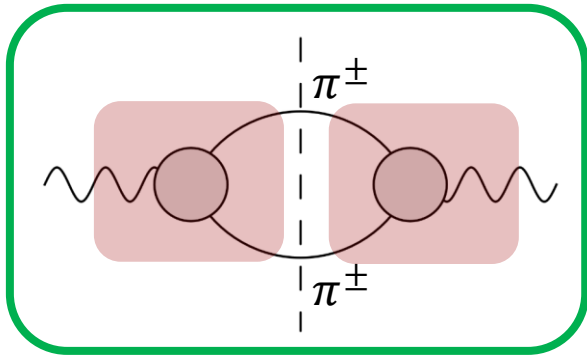
- $\pi\pi$ channel is the dominant source of uncertainty in HVP
- Many discrepancies remain between $e^+e^- \rightarrow \pi^+\pi^-$ experiments



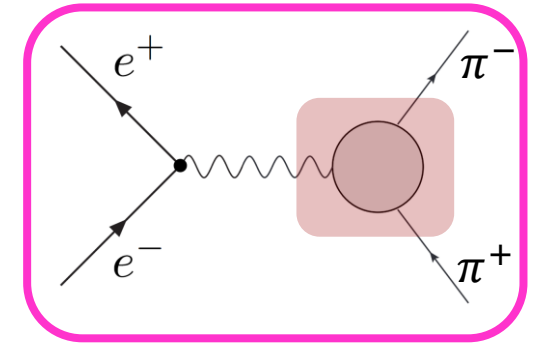
$$a_\mu^{\text{HVP}(\pi\pi)} = \frac{m_\mu^2}{4\pi^2} \int_{s_{\text{thr}}}^\infty \frac{\hat{K}(s)}{s} \sigma(e^+e^- \rightarrow \pi^+\pi^- (+\gamma))$$



- $\pi\pi$ channel is the dominant source of uncertainty in HVP
- Many discrepancies remain between $e^+e^- \rightarrow \pi^+\pi^-$ experiments
- How can we use theory inputs to shed light on these puzzles?



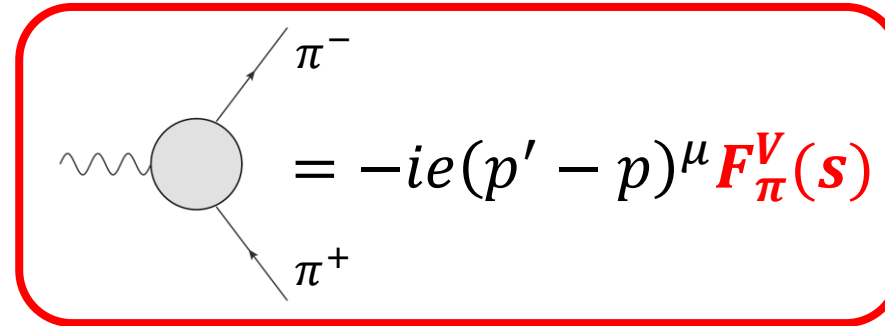
$$a_{\mu}^{\text{HVP}(\pi\pi)} = \frac{m_{\mu}^2}{4\pi^2} \int_{s_{\text{thr}}}^{\infty} \frac{\hat{K}(s)}{s} \sigma(e^+e^- \rightarrow \pi^+\pi^- (+\gamma))$$



$$= -ie(p' - p)^{\mu} F_{\pi}^V(s)$$

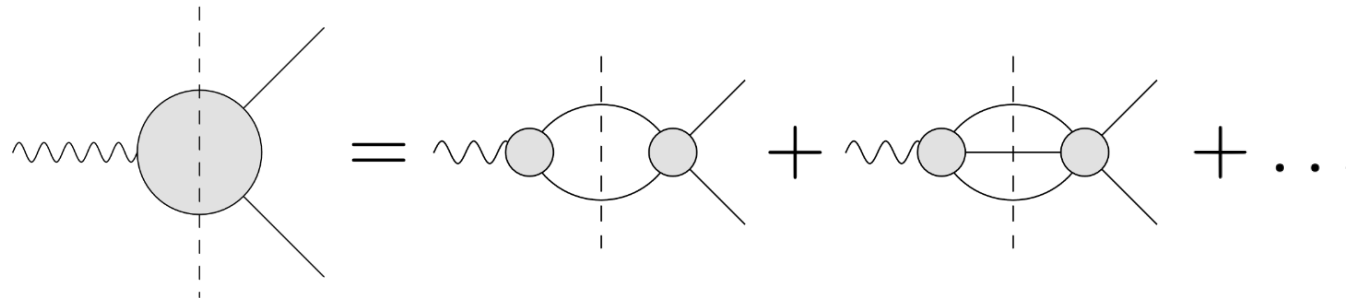
PION VECTOR FORM FACTOR

THE PION VECTOR FORM FACTOR (VFF)



A Feynman diagram showing a wavy line (photon) entering a grey circular vertex from the left. Two straight lines exit the vertex to the right: the upper one is labeled π^- and the lower one is labeled π^+ . The entire diagram is enclosed in a red rounded rectangle. To the right of the diagram is the equation $= -ie(p' - p)^\mu \mathbf{F}_\pi^V(s)$, where the vector \mathbf{F}_π^V is written in red.

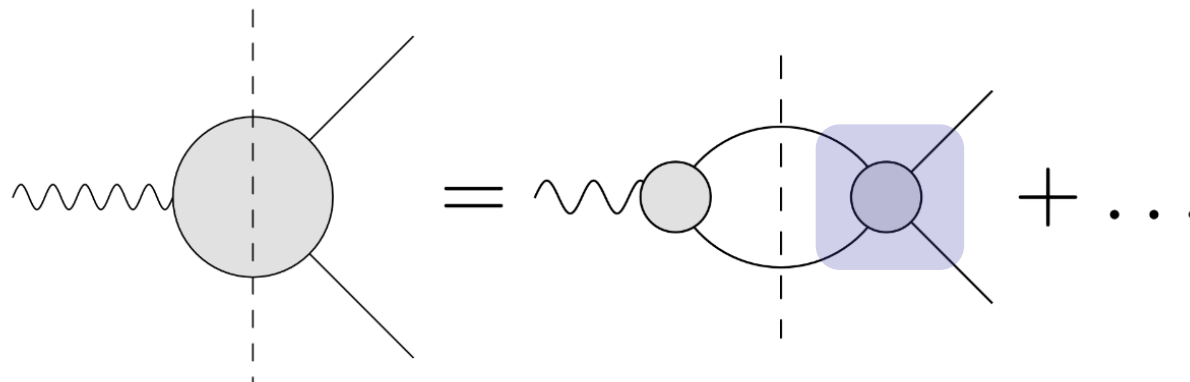
- **Unitarity:** The VFF can be decomposed into intermediate states contributions
- **Analiticity:** The knowledge of the VFF above threshold implies its knowledge everywhere
- With theory input on the channels ($\pi^+\pi^-$, $\pi^0\gamma$, $3\pi[\omega, \dots]$, $4\pi[\pi^0\omega, \dots]$, etc.) we can write a **model-independent parameterized closed form** of the VFF that we can **fit to data**



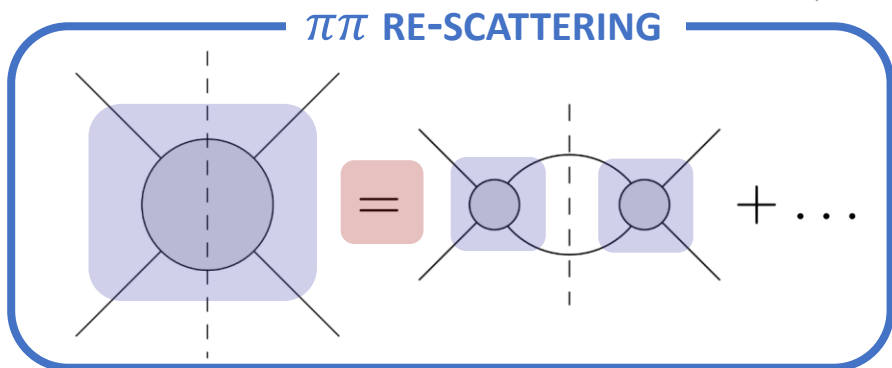
A diagrammatic equation showing the decomposition of the pion vector form factor. On the left is the full vertex diagram (a grey circle with a wavy line and two outgoing lines). This is set equal to a sum of diagrams. The first term is a diagram with a wavy line entering a grey circle, which is connected to another grey circle via two arcs (representing a $\pi^+\pi^-$ intermediate state), which then connects to a final grey circle with two outgoing lines. The second term is a similar diagram but with a horizontal line through the middle of the arcs (representing a $\pi^0\gamma$ intermediate state). This is followed by a plus sign and an ellipsis, indicating further terms in the series.

MODEL-INDEPENDENT DESCRIPTION OF THE PION VFF

- Decomposition of the VFF in terms of intermediate states



Caprini, Colangelo, Leutwyler,
Eur.Phys.J.C 72 (2012) 1860



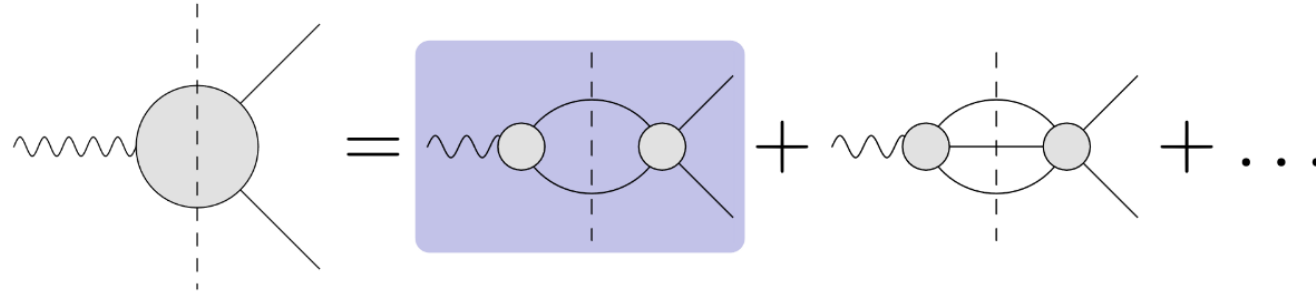
Depends only on the *elastic* phase shift $\delta_1^1(s)$ of the *P-wave* in the *isospin* $I = 1$ channel

$$= -ie(p' - p)^\mu F_\pi^V(s)$$

$$t_1^1(s) = \frac{\sin \delta_1^1(s) e^{i\delta_1^1(s)}}{\sigma_\pi(s)} + \dots$$

Roy equations

→ Solution for $\delta_1^1(s)$ below ≈ 1.15 GeV

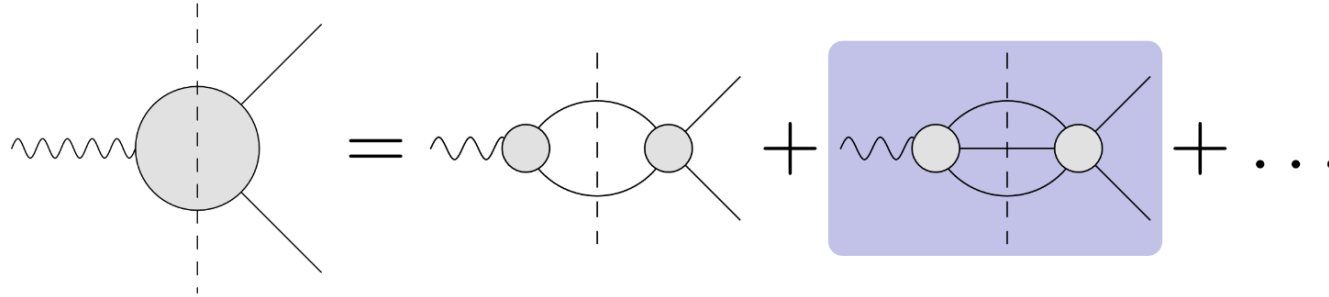


Colangelo, Hoferichter,
Stoffer, JHEP 02 (2019) 006

$$F_{\pi}^V(s) = \Omega_1^1(s) \times G_{\omega(\phi)}(s) \times G_{\text{in}}(s)$$

- Omnès function with elastic $\pi\pi$ -scattering P -wave phase shift $\delta_1^1(s)$ as input:

$$\Omega_1^1(s) = \exp \left\{ \frac{s}{\pi} \int_{4M_{\pi}^2}^{\infty} ds' \frac{\delta_1^1(s')}{s'(s' - s)} \right\}$$



Colangelo, Hoferichter,
Stoffer, JHEP 02 (2019) 006

$$F_{\pi}^V(s) = \Omega_1^1(s) \times G_{\omega(\phi)}(s) \times G_{\text{in}}(s)$$

- Isospin-breaking 3π intermediate state: negligible apart from ω and ϕ resonances (mixing with the ρ resonance)

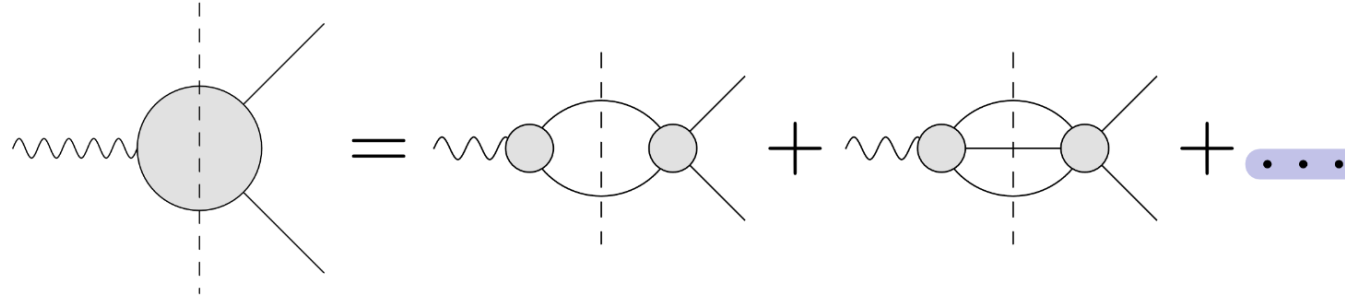
$$G_{\omega}(s) = 1 + \frac{s}{\pi} \int_{9M_{\pi}^2}^{\infty} ds' \frac{\text{Im} g_{\omega}(s')}{s'(s' - s)} \left(\frac{1 - \frac{9M_{\pi}^2}{s'}}{1 - \frac{9M_{\pi}^2}{M_{\omega}^2}} \right)^4$$

Colangelo, Hoferichter, Kubis,
Stoffer, JHEP 10 (2022) 032

$$g_{\omega}(s) = 1 + \epsilon_{\omega} \frac{s}{(M_{\omega} - \frac{i}{2}\Gamma_{\omega})^2 - s}$$

+ additional terms $\propto \text{Im} \epsilon_{\omega}$ to account for $\pi^0 \gamma$ effects

+ additional terms for ϕ resonance



Colangelo, Hoferichter,
Stoffer, JHEP 02 (2019) 006

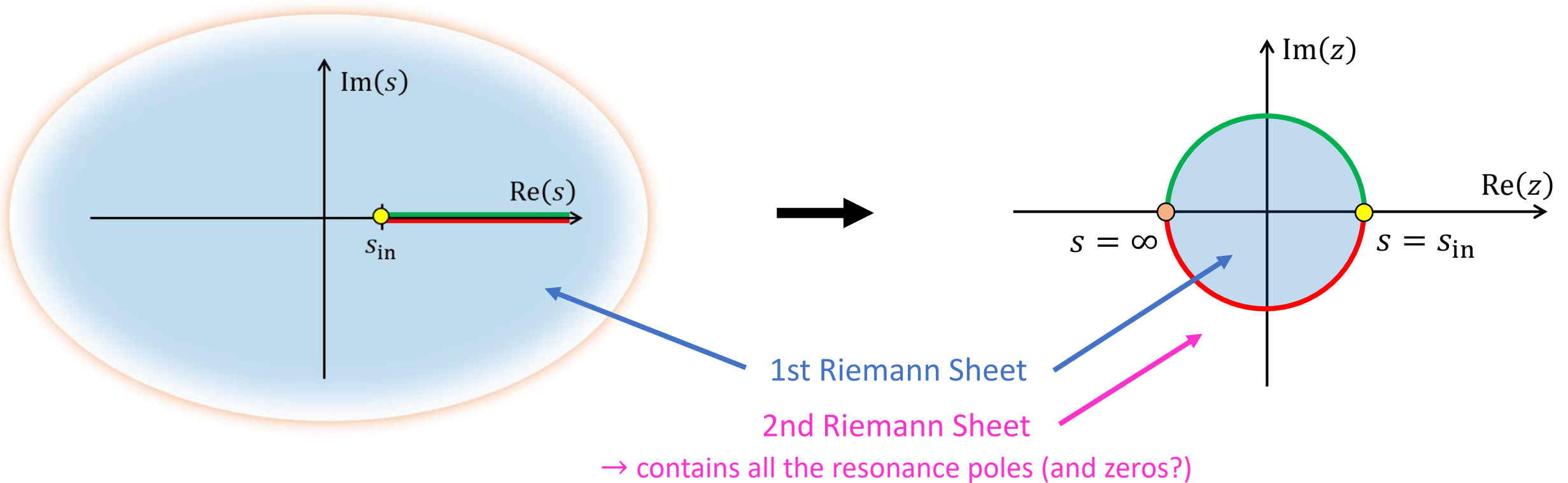
$$F_{\pi}^V(s) = \Omega_1^1(s) \times G_{\omega(\phi)}(s) \times G_{\text{in}}(s)$$

- Heavier intermediate states: 4π (mainly $\pi^0\omega$), $K\bar{K}$, ...
- Description with a cut starting at the $\pi^0\omega$ threshold: $s_{\text{in}} = (M_{\pi^0} + M_{\omega})^2$
- P -wave behavior imposed near the threshold

$$\text{Im } G_{\text{in}}(s) \sim (s - s_{\text{in}})^{3/2}$$

→ **Need an explicit parameterization of G_{in}**

- Implements **branch cut + asymptotic behavior** $z(s) = \frac{\sqrt{s_{\text{in}} - s_c} - \sqrt{s_{\text{in}} - s}}{\sqrt{s_{\text{in}} - s_c} + \sqrt{s_{\text{in}} - s}}$



- Thus, the inelastic factor is conveniently written as a **function of $z(s)$**

- In our previous analyses, G_{in} was described as a **polynomial in z** :

$$G_{\text{in}}(z) = 1 + \sum_{k=1}^N \left(z^k - z_0^k \right)$$

*Colangelo, Hoferichter,
Stoffer, JHEP 02 (2019) 006*

which is able to **fit the data up to $\approx 1\text{GeV}$ for degrees $N = 2 \dots 6$**

- Our last analysis investigated the **impact of the zeros in the first Riemann Sheet**

- Excluding these zeros resolves some instabilities and variability of the fits with N
- Excluding zeros does not degrade the goodness of fit
- The fitted zeros were already excluded by analyticity constraints
- Zeros are excluded by χPT : all the zeros must be outside of the range of validity of χPT

Leplumey, Stoffer, arXiv:2501.09643

Leutwyler, Continuous advances in QCD (2002) 23-40

- In addition, we also implemented a **zero-free semi-model-dependent description of the inelasticities** (dispersively improved Gounaris-Sakurai functions) to fit the high-energy data (up to 3 GeV) and check consistency

Ruiz Arriola, Sanchez-Puertas, arXiv 2403.07121

*Gounaris, Sakurai,
Phys.Rev.Lett 21 (1968) 244-247*

NEW IMPLEMENTATION OF THE INELASTICITIES

Alternative descriptions of the VFF use a conformal description from the elastic threshold $4M_\pi^2$ and incorporate an **outer function** (OF)

$$F_\pi^V(s) = \frac{1}{\phi(z_{\pi\pi})} \sum_{k=1}^N a_k z_{\pi\pi}^k$$

*Buck, Lebed,
Phys.Rev.D 58 (1998) 056001*

*Ananthanarayan, Caprini, Imsong,
Phys.Rev.D 83 (2011) 096002*

With the motivation of incorporating **dispersive bounds** written as

$$\frac{1}{2\pi i} \int_C \frac{dz}{z} |\phi(z) F_\pi^V(z)|^2 \leq 1 \quad \longrightarrow \quad \sum_{k=0}^N |a_k|^2 \leq 1$$

Such an OF can improve the convergence of the conformal expansion by setting this orthogonality constraint

One common choice of OF is the following

- $s_c = -1 \text{ GeV}^2$: central point for conformal transformation
- s_0 : branch cut threshold
- $Q^2 = -q^2 = -1 \text{ GeV}^2$: point where the bound is evaluated

$$\phi(z) \propto \left[\sqrt{1 - \frac{s_c}{s_0}}(1 - z) + (1 + z) \right]^{-1/2} \left[\sqrt{1 + \frac{Q^2}{s_0}}(1 + z) + \sqrt{1 - \frac{s_c}{s_0}}(1 - z) \right]^{-3}$$

- The initial motivation is a dispersive bound on the $\pi\pi$ channel of HVP

$$\frac{1}{\pi} \int_0^\infty ds \frac{\Pi_J^T(s)|_{\pi\pi}}{(s - q^2)^3} \leq \left[\frac{1}{2} \frac{\partial^2 \Pi_J^T}{\partial^2 (q^2)^2} \right]_{\text{pQCD}}$$

*Buck, Lebed,
Phys.Rev.D 58 (1998) 056001*

*Kirk, Kubis, Reboud, van Dyk,
Phys.Lett.B 861 (2025) 139266*

- This OF mainly contains information on the **two-body kinematics**
- Supplemented by Blaschke factor corrections to remove sub-threshold singularities and correct the behavior at threshold and infinity

- The dispersive bound is saturated only at $\approx 45\%$, and therefore cannot be used to constrain any data fit
- Still, this OF is relevant to describe the **effective two-body kinematics** at $\pi^0\omega$ threshold

$$G_{\text{in}}(z) = \frac{1}{\phi(z)} P_N(z)$$

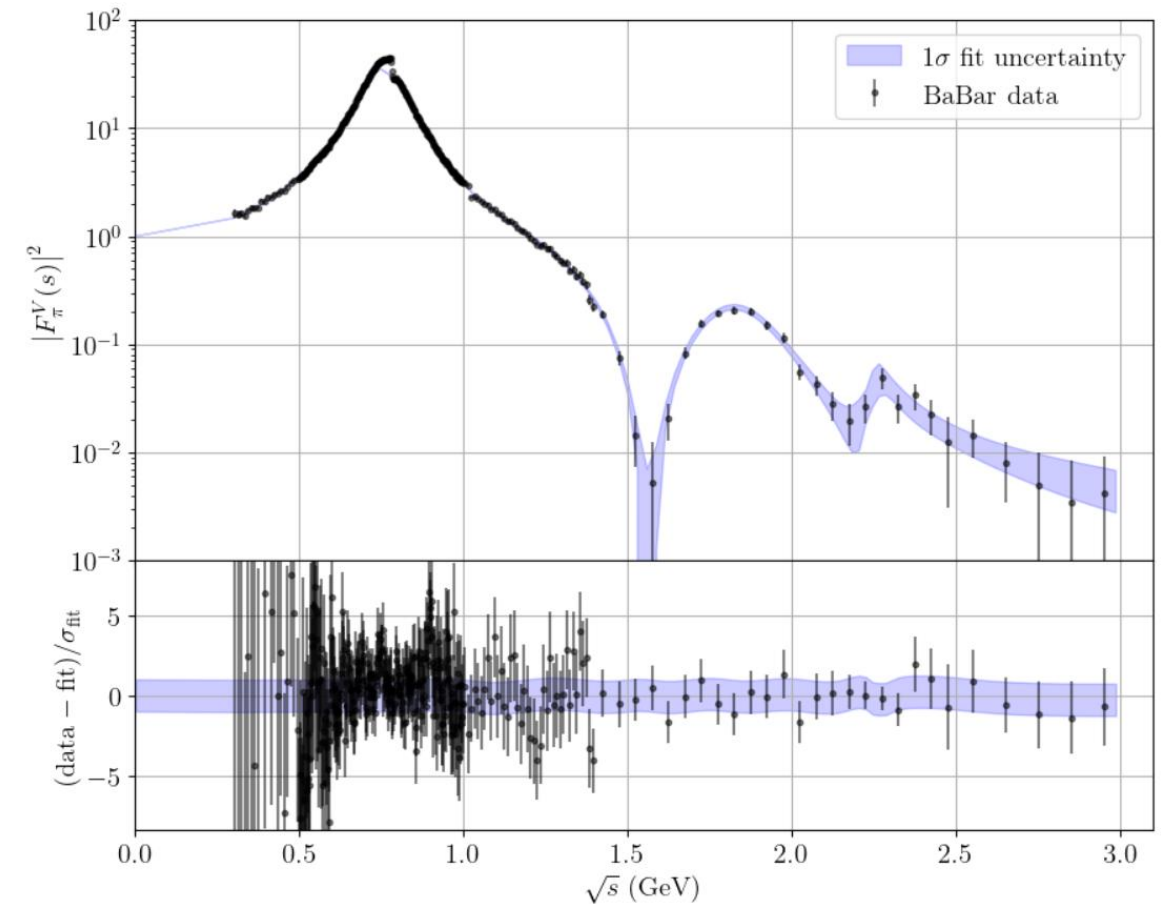
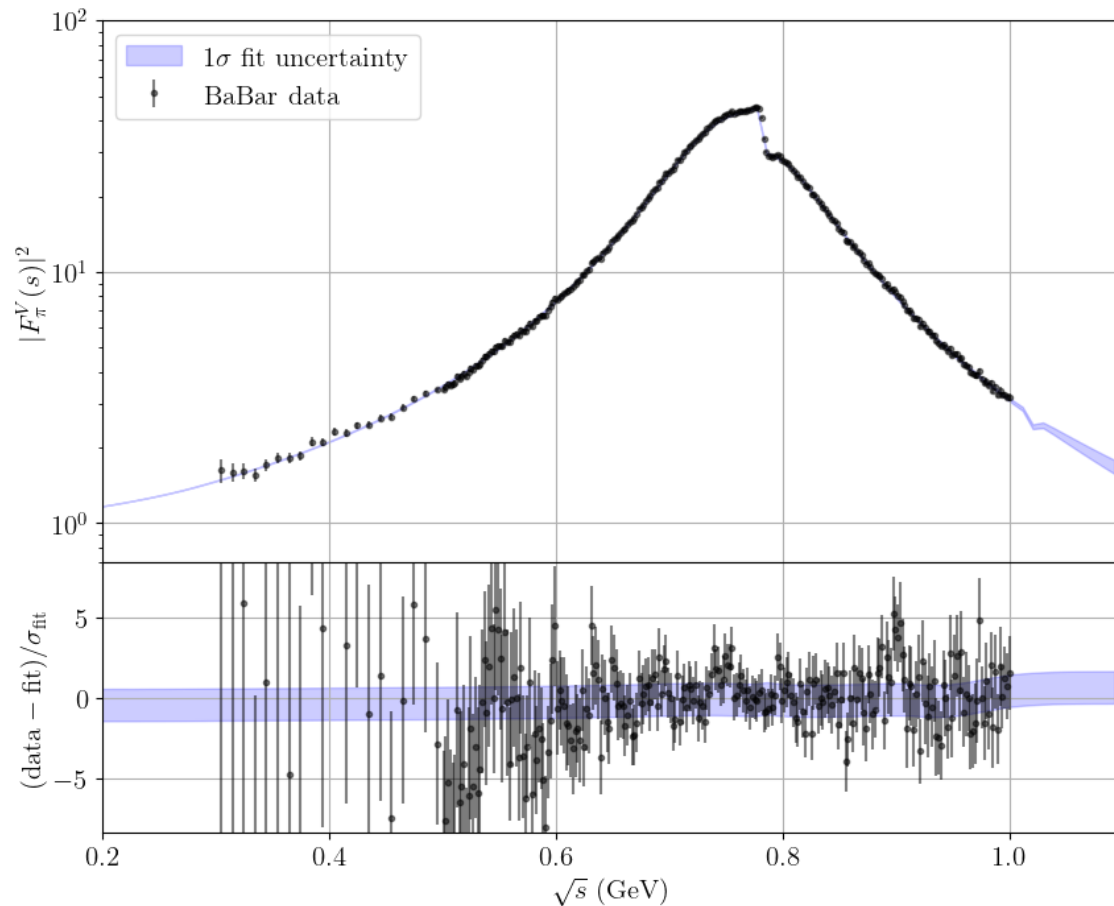
- It can be further complemented by the introduction of **explicit poles** in order to describe the resonances visible in multi-GeV data

$$G_{\text{in}}(z) = \frac{1}{\phi(z)} \frac{P_N(z)}{\prod_j (z - z_j)(z - z_j^*)}$$

*Kirk, Kubis, Reboud, van Dyk,
Phys.Lett.B 861 (2025) 139266*

FIT OF THE VFF

- Different fits are performed:
 - Fits to sub-GeV data only without explicit resonance poles in the parameterization (e.g. left)
 - Full-range fits with three explicit resonance poles in the parameterization (e.g. right)



IMPROVED METHODOLOGY FOR PARAMETER INFERENCE

$$F_{\pi}^V(s) = \Omega_1^1(s) \times G_{\omega(\phi)}(s) \times G_{\text{in}}(s)$$

2 parameters:
Value of $\delta_1^1(s)$ at 2
particular points

3 parameters:
 M_{ω} , $\text{Re } \epsilon_{\omega}$, $\text{Im } \epsilon_{\omega}$ (+
 $\text{Re } \epsilon_{\phi}$, $\text{Im } \epsilon_{\phi}$ when ϕ visible in
data)

$N - 1$ parameters:
 c_2, \dots, c_N
(+ $2 \times n_{\text{poles}}$ for full-range fits)

- Multiple fits to individual experiments:
 - Direct-scan: SND06, CMD-2, SND20, CMD-3
 - Radiative-return: BaBar, KLOE, BESIII
- Use of unbiased fitting to avoid the d'Agostini bias

*NNPDF Collaboration,
JHEP 05 (2010) 075*

*D'Agostini, Nucl.Instrum.Meth.A
362 (1995) 487-498*

The inference is based on a χ^2 -like negative log-likelihood:

$$\chi^2 = \chi_{\text{data}}^2 + \chi_{\text{EL}}^2 + \chi_{\text{zeros}}^2 + \chi_{\text{syst}}^2$$

- Data constraint: $\chi_{\text{data}}^2 = [\sigma(s_i, \theta) - \sigma_i]^T \Sigma^{-1} [\sigma(s_i, \theta) - \sigma_i]$
- Eidelman-Łukaszuk bound: upper bound on the inelastic phase of the VFF close to the inelastic threshold, constrained by external experimental data

Colangelo, Hoferichter, Kubis, Stoffer, JHEP 10 (2022) 032

Eidelman, Łukaszuk, Phys.Lett.B 582 (2004) 27-31

- Sum-rule constraint for the absence of zeros $\frac{\sqrt{s_{\text{in}}}}{\pi} \int_{s_{\text{in}}}^{\infty} \frac{ds}{(s - s_{\text{in}})^{3/2}} \log \left| \frac{G_{\text{in}}(s)}{G_{\text{in}}(s_{\text{in}})} \right| = 0$

Leplumey, Stoffer, arXiv:2501.09643

- Prior constraints on the model systematics parameters
 - Roy equation parameters, Γ_{ω} , M_{ϕ} , Γ_{ϕ} , s_c , asymptotic extrapolation of δ_1^1

- Separate fits are performed for each value of N (degree of the conformal polynomial)
- Under Gaussianity, we derive the posterior for each fit separately against data D :
 - Studies have been performed to ensure Gaussianity hypothesis is nearly correct and conservative in our case

$$(\theta|D, N) \sim \mathcal{N}(\hat{\theta}_N, \hat{\Sigma}_N)$$

- The posteriors are then marginalized over N

$$p(\theta|D) = \sum_N p(\theta|D, N)p(N|D)$$

- If N has a flat (or exponential) prior, then one can show that

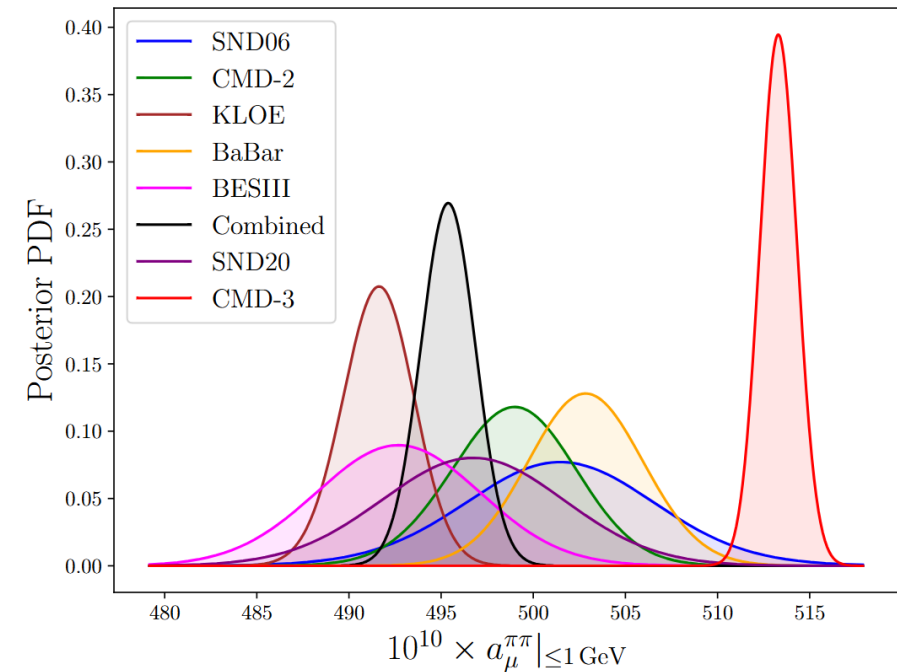
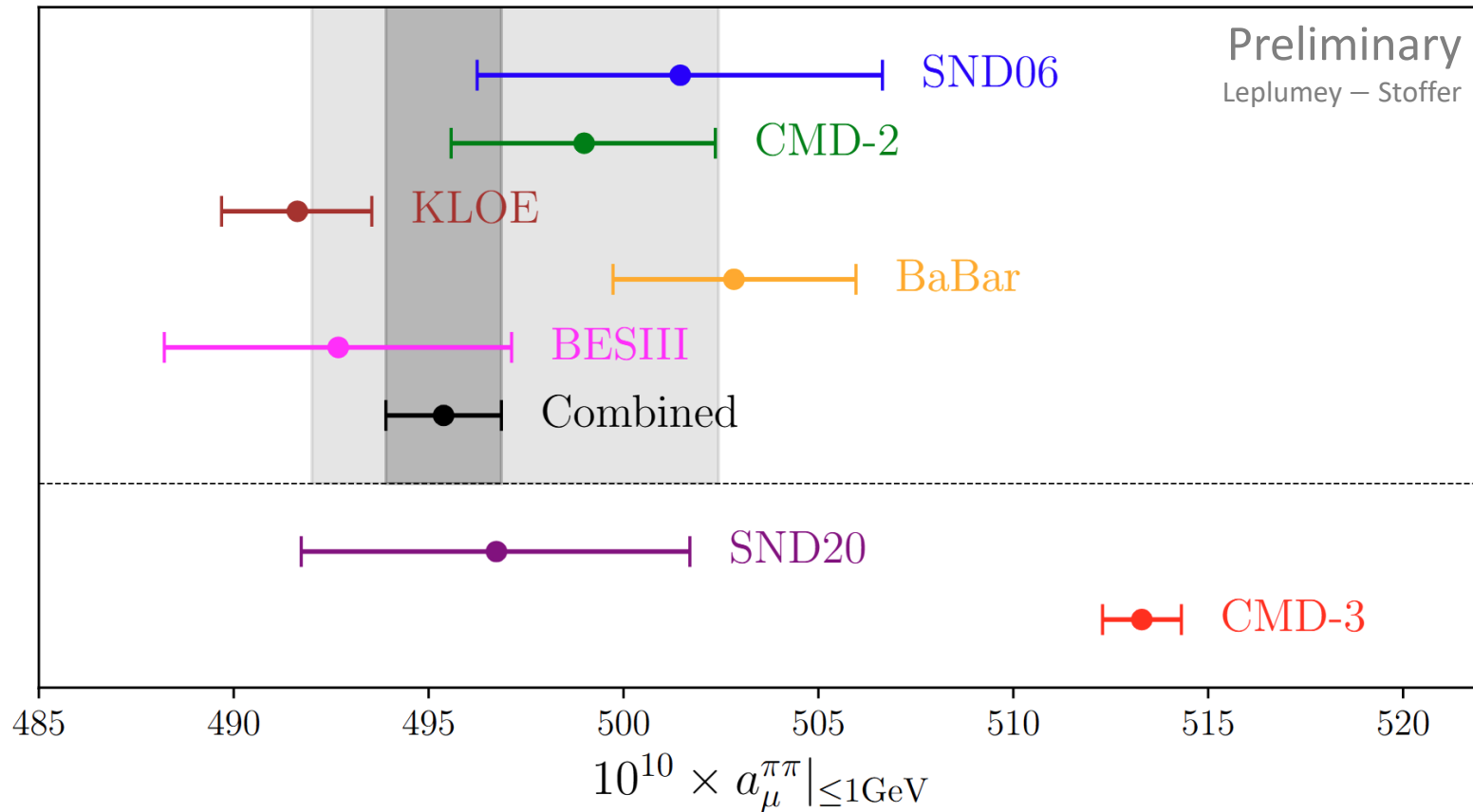
$$p(N|D) \simeq \exp \left(-\frac{1}{2} \left(\chi_N^2(\hat{\theta}_N) + \alpha N \right) \right)$$

- $\alpha \sim \log |D|$ would hold for very large dataset (Bayesian information)
- Smaller α tend to be more conservative & accurate if none of the models is exact (e.g. $\alpha = 2$ for Akaike information)
- We choose $\alpha = 1$ for our nominal inference, which penalizes the addition of one parameter by one χ^2 unit

RESULTS FOR $a_{\mu}^{\text{HVP,LO}}[\pi\pi, e^+e^-]$

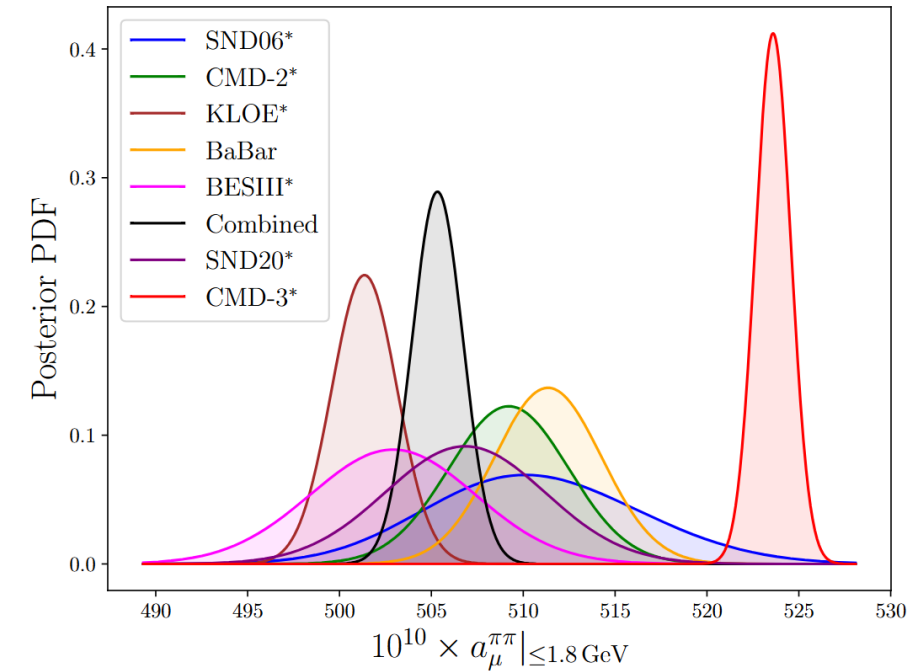
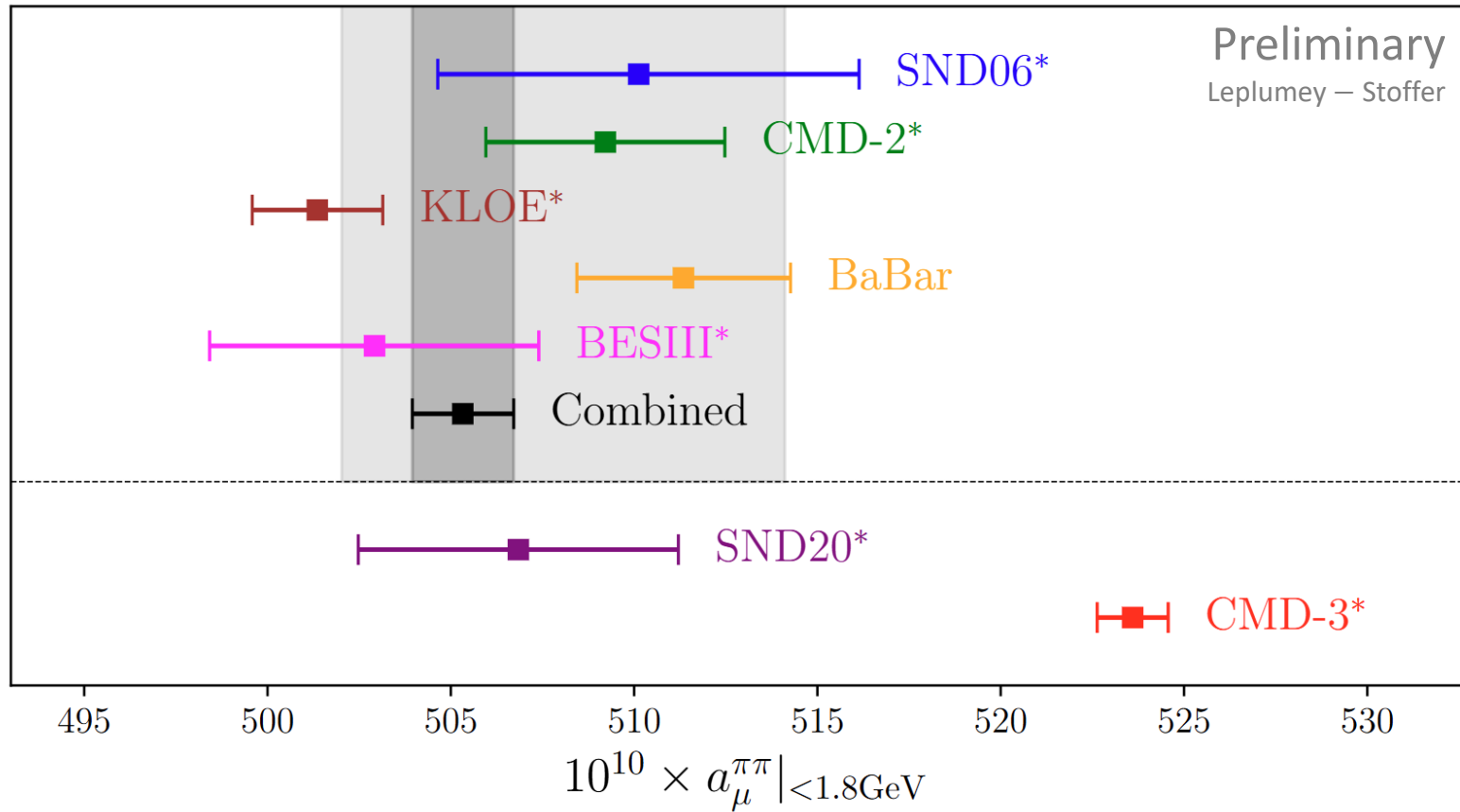
RESULT FOR $a_\mu^{\text{HVP,LO}}[\pi\pi, e^+e^-]$ BELOW 1GeV

- All the datasets are truncated at 1 GeV
- No resonance poles are explicitly introduced in the inelastic factor



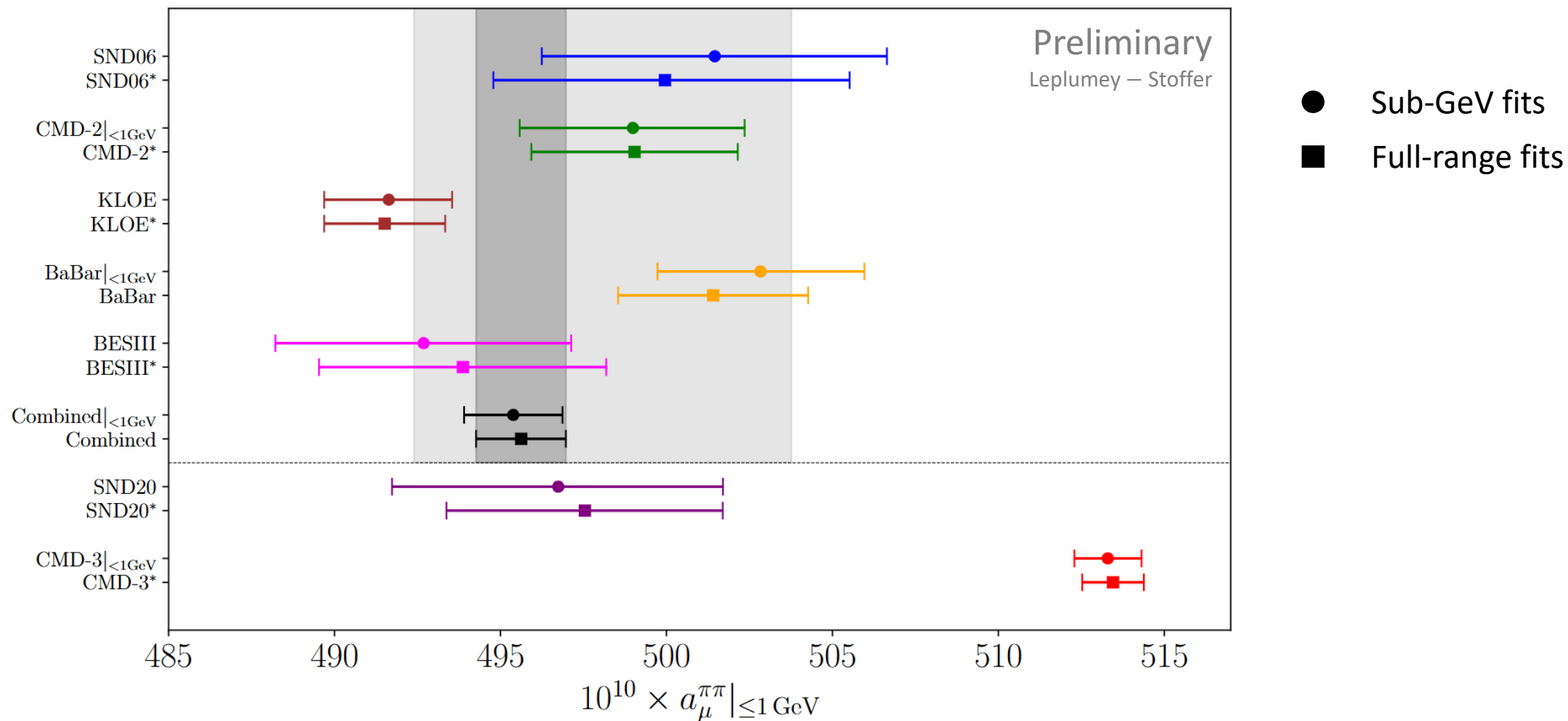
RESULT FOR $a_\mu^{\text{HVP,LO}}[\pi\pi, e^+e^-]$

- All the datasets marked with a * are combined with BaBar data above 1.4 GeV
- 3 resonance poles are explicitly fitted in the parameterization (ρ' , ρ'' and ρ''')



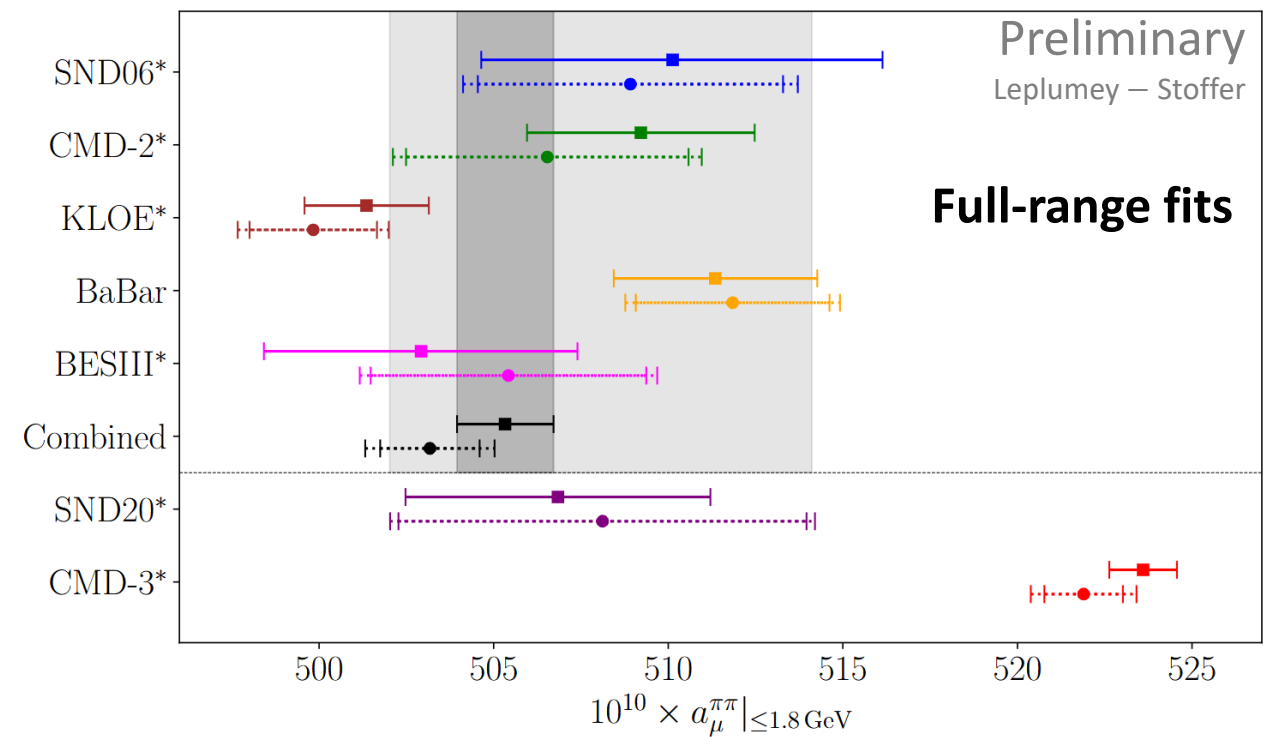
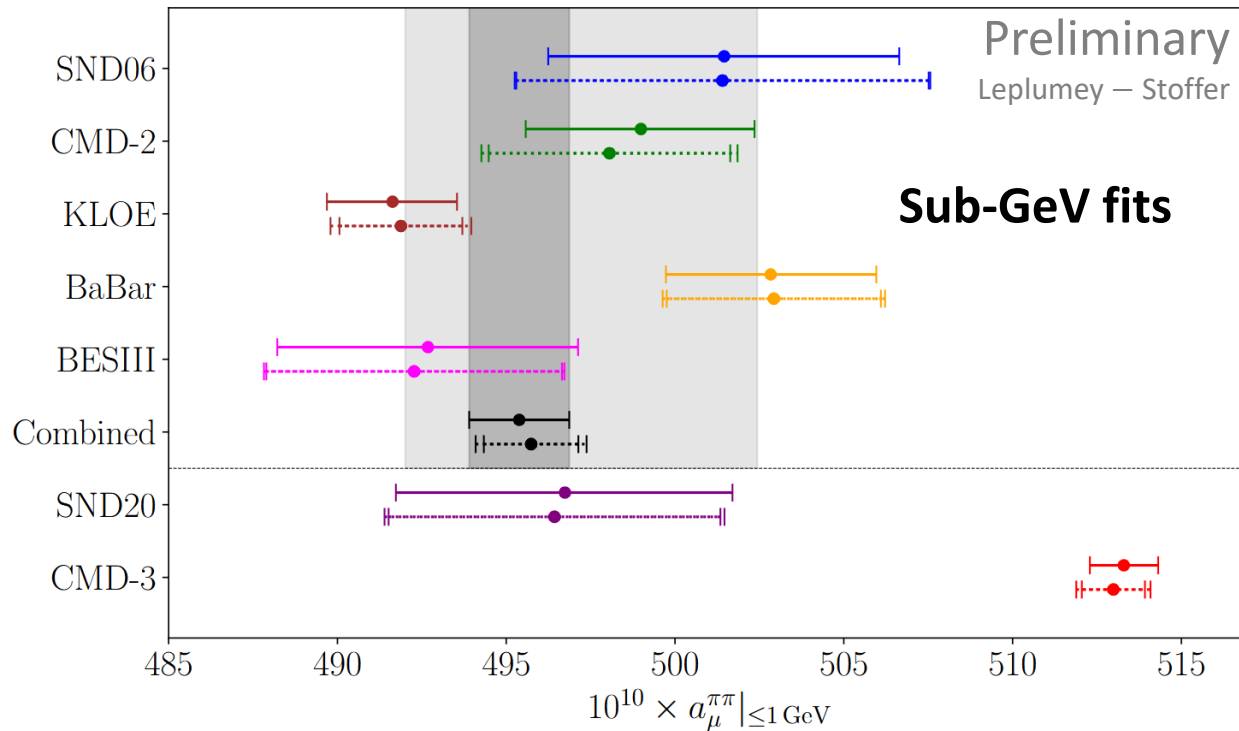
CONSISTENCY IN $a_\mu^{\text{HVP,LO}}[\pi\pi, e^+e^-]$ BELOW 1GeV

- Very good consistency is observed between sub-GeV and multi-GeV fits!



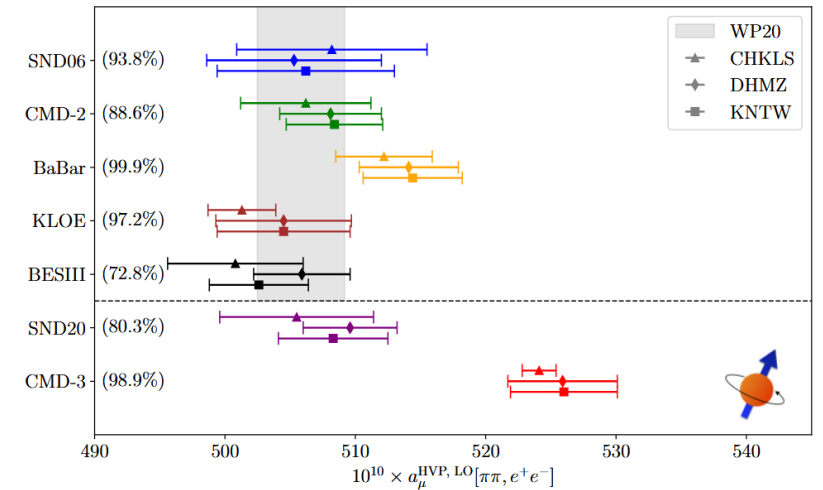
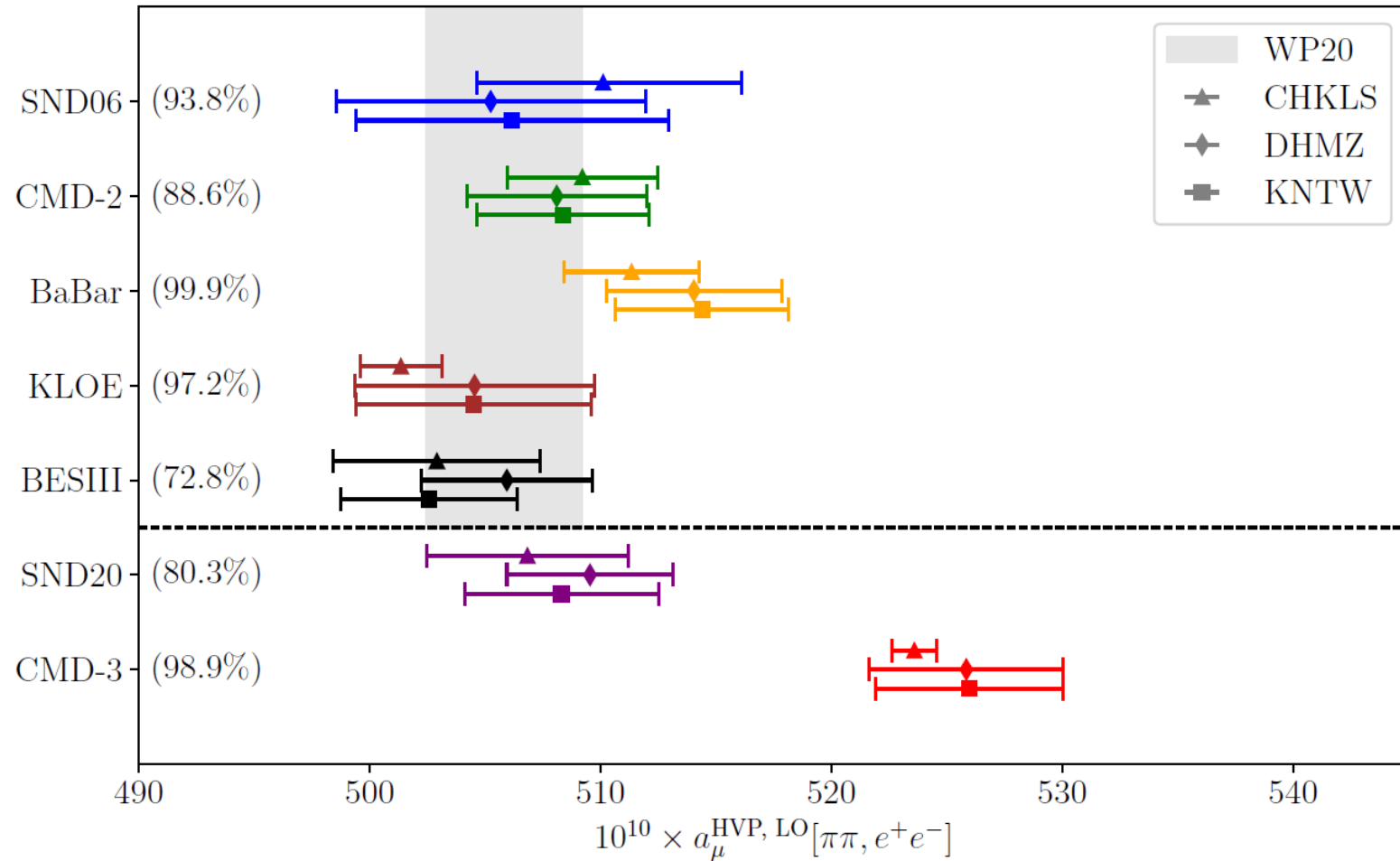
COMPARISONS WITH OUR PREVIOUS ANALYSIS

- Very good consistency is observed with our previous analysis
- The new analysis allows better interpretability of the credible intervals



- New analysis (preliminary)
- Previous analysis (arXiv:2501.09643)

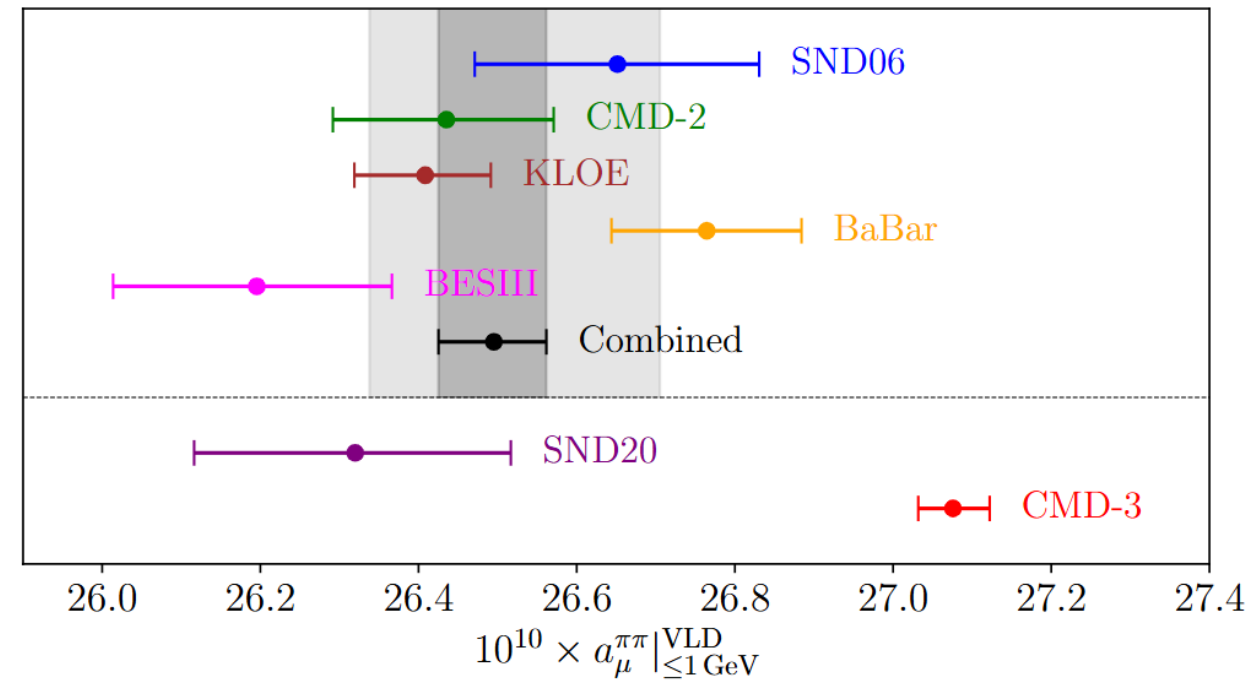
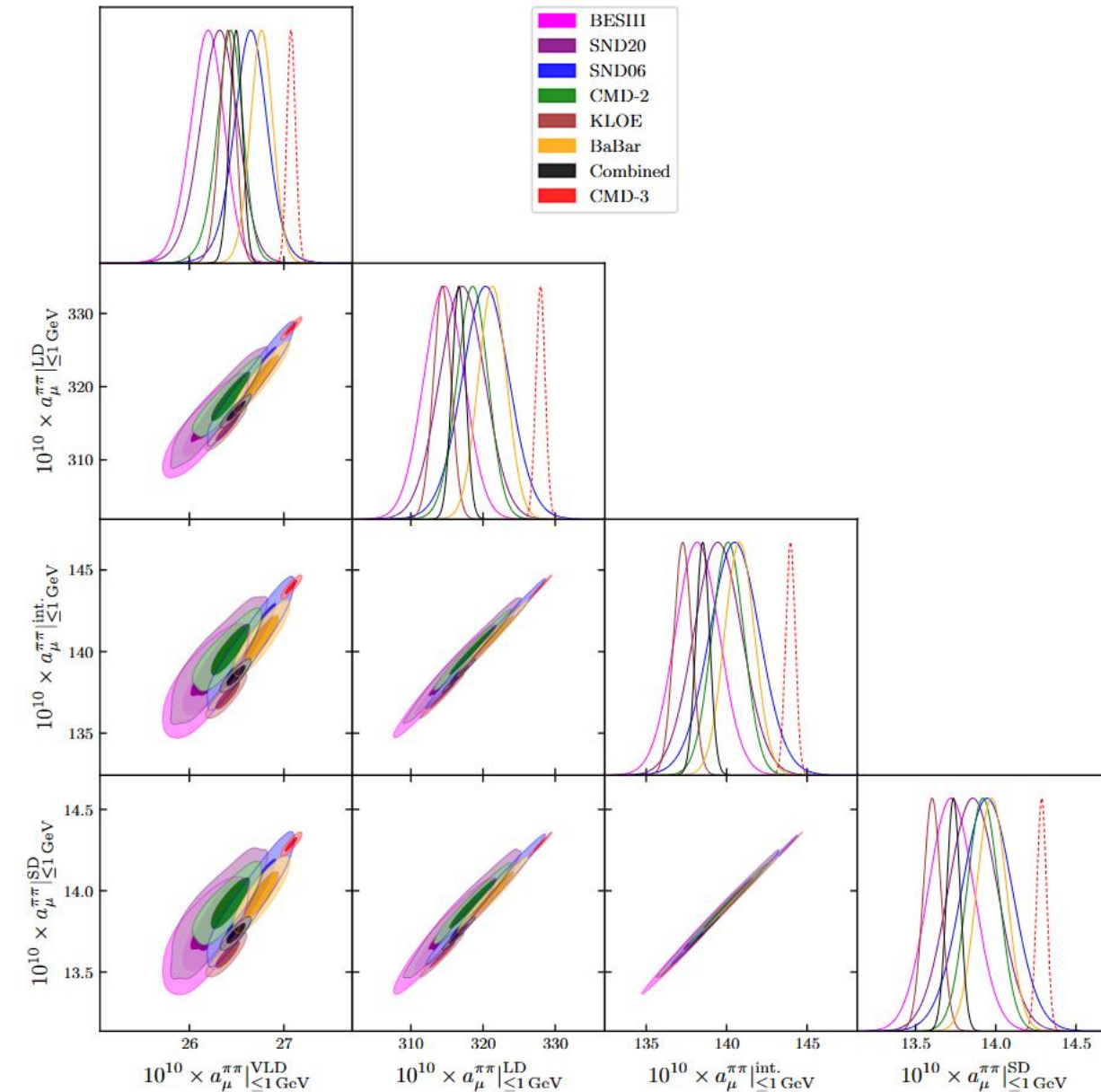
- Our results remain compatible with other approaches



WP25: Fig. 26

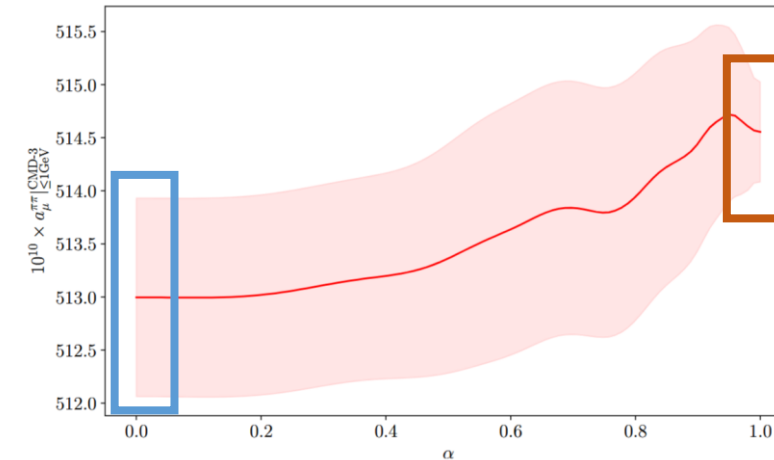
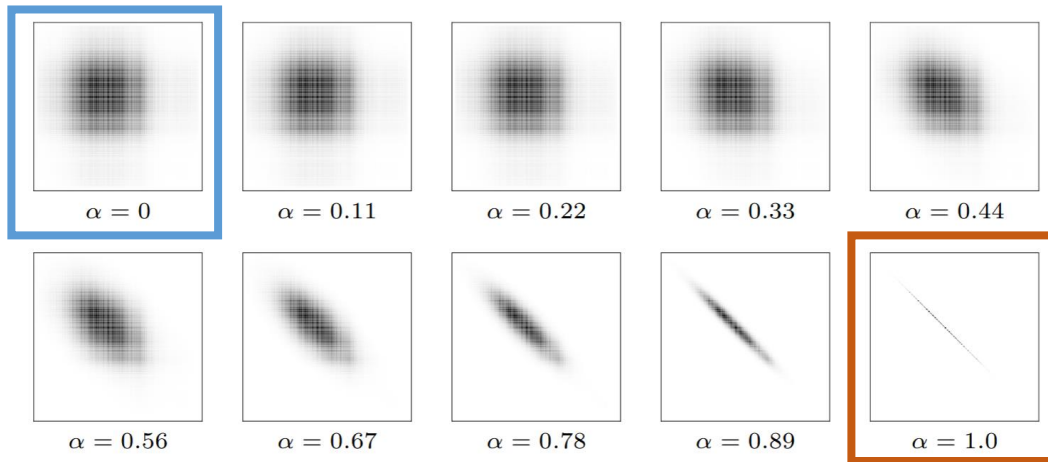
EUCLIDEAN WINDOWS

- The different euclidean windows are actually very **correlated by the data fit**
- Therefore, **the discrepancies propagate to all the windows**, even at very long distance!



- Some concerns have been raised about the impact of **correlations in CMD-3 data**
 - For **direct integration**, **fully correlated covariance** is clearly the **most conservative**
 - However, it is less clear *a priori* whether this choice is conservative or not in our framework

- In our last analysis, we implemented a “decorrelation scheme” to evaluate this:



Leplumey, Stoffer,
arXiv:2501.09643

- Smaller correlations lead to **higher value of $a_{\mu}^{\pi\pi}$** and **smaller uncertainty!**
 - Full correlations allow global scale effects \rightarrow analyticity constraints seem to pull the VFF down
 - Zero/negative correlations constrain the fit to be closer to the central values of the data points

- To assess this issue, we tried **tuning the covariance *a posteriori*** to get the largest posterior uncertainty in $a_{\mu}^{\pi\pi}$ (\rightarrow expected to be the most conservative choice)

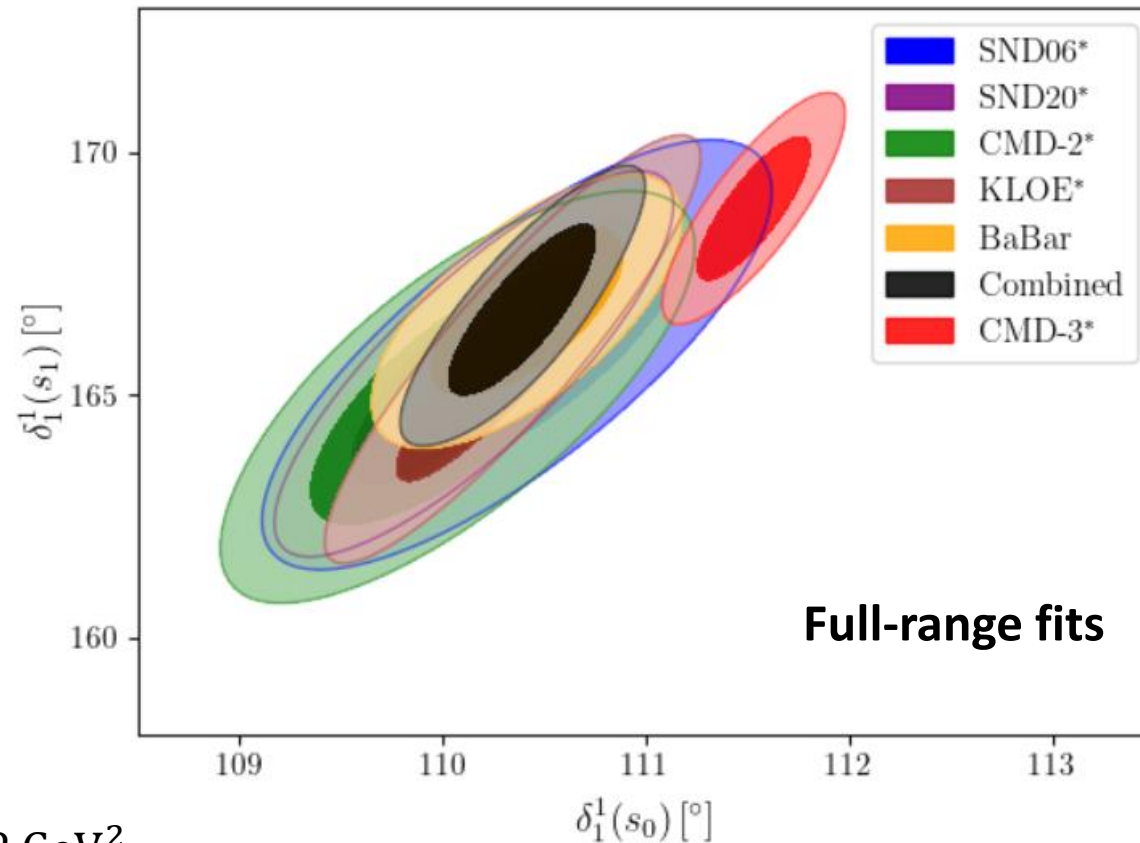
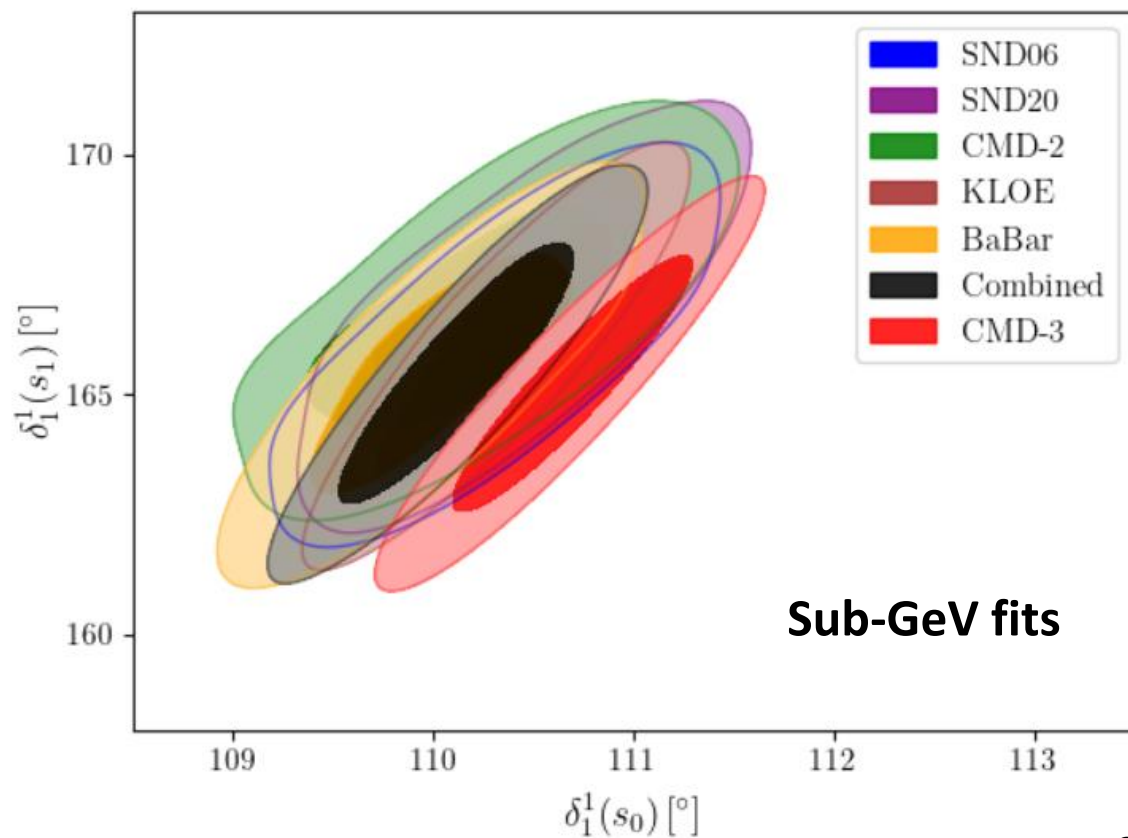
$$\text{Corr}(\sigma_i, \sigma_j) = \text{sign} \left(\frac{\partial a_{\mu}^{\pi\pi}}{\partial \sigma_i} \times \frac{\partial a_{\mu}^{\pi\pi}}{\partial \sigma_j} \right)$$

- However, the *a posteriori* conservative covariance **depends on the starting point**
 - Starting from the fully correlated best-fit point, the conservative option is consistently the fully correlated covariance matrix
 - Starting from the uncorrelated best-fit point, the conservative option contains **anti-correlations** between different energy regions, but **the overall uncertainty remains smaller**
- Without a clear prescription yet, we decided to **stick to the full corr. prescription**
 - This makes the interpretation and comparison with other results easier
 - This choice **does not overestimate the discrepancy** with other experiments

RESULTS FOR OTHER OBSERVABLES

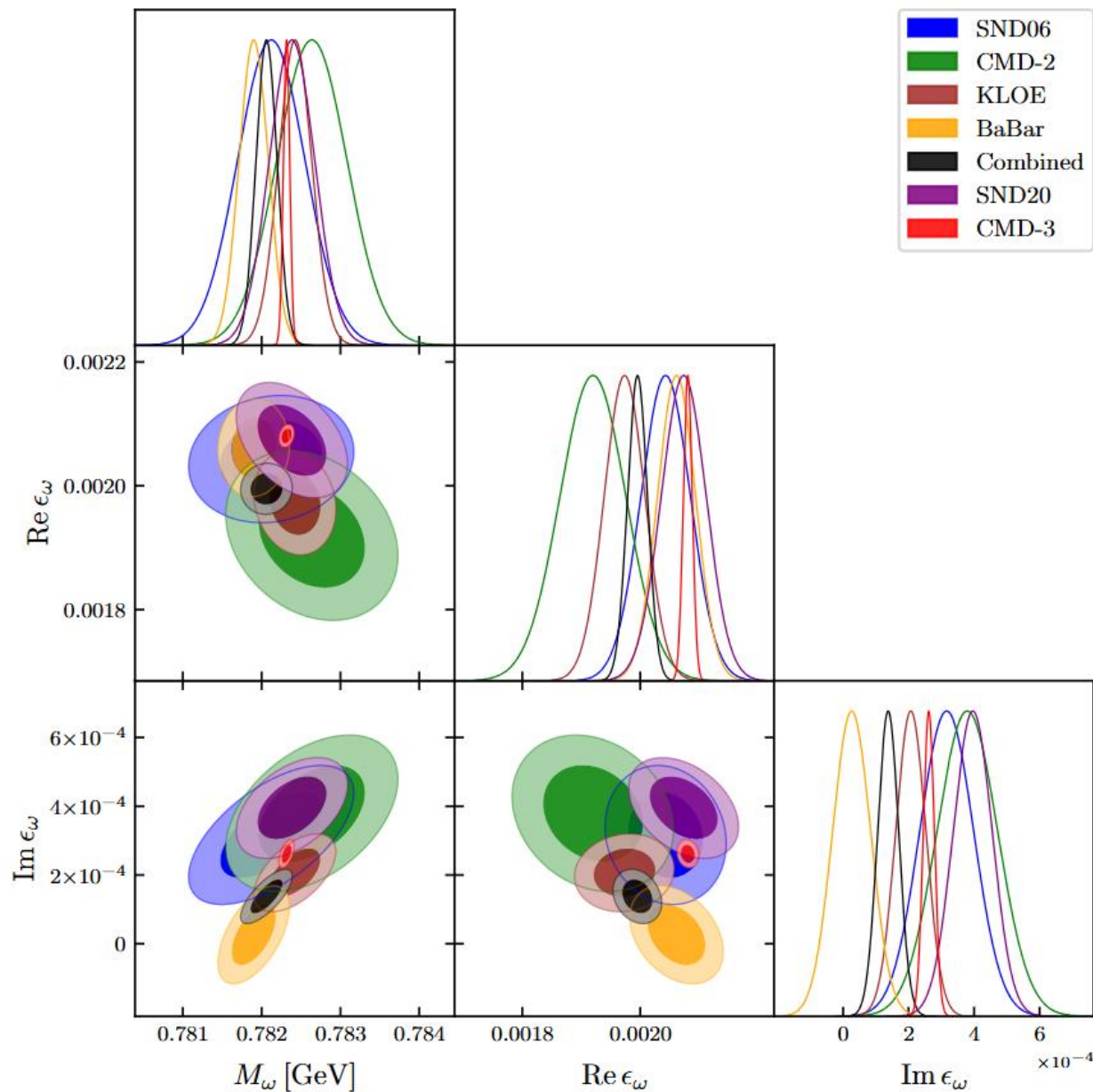
RESULT FOR THE ELASTIC PHASE SHIFT

- The elastic contributions are described by the elastic phase shift δ_1^1
- Small disagreements are found between CMD-3 and other experiments



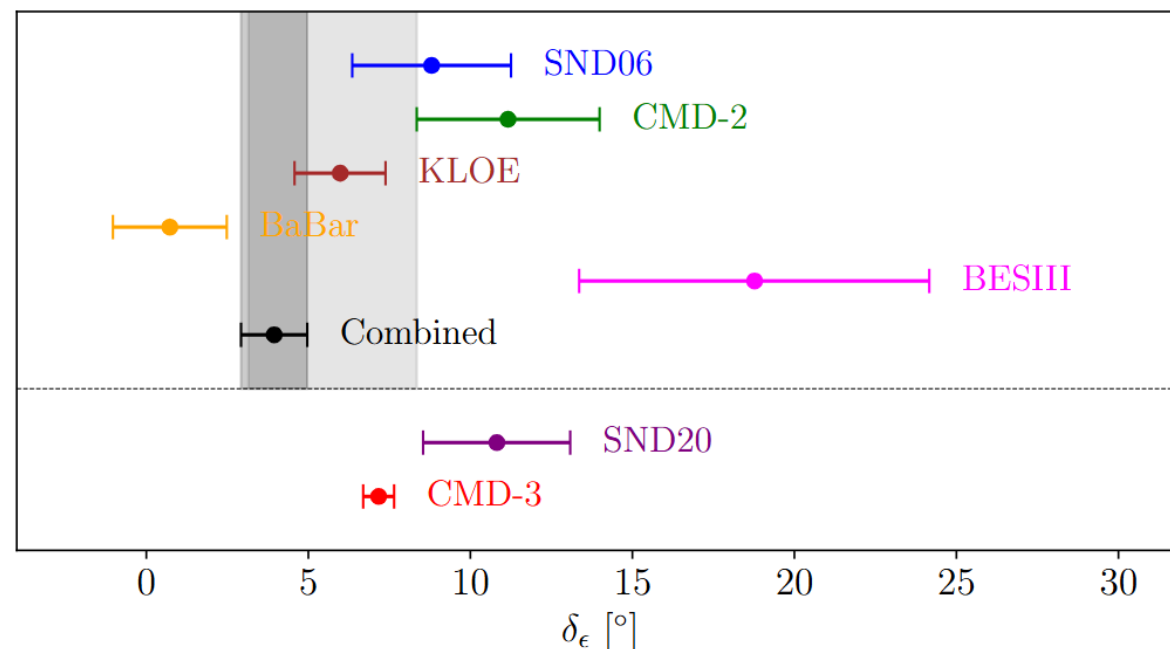
$$s_0 = 0.8 \text{ GeV}^2$$
$$s_1 = 1.15 \text{ GeV}^2$$

RESULT FOR THE ω PARAMETERS



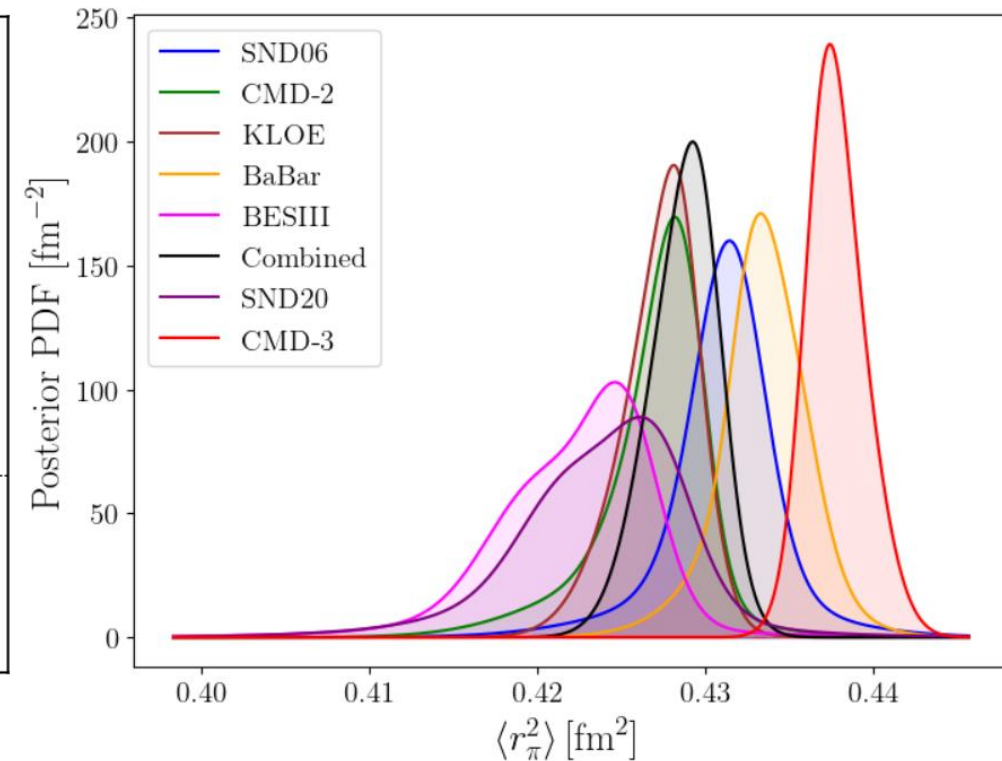
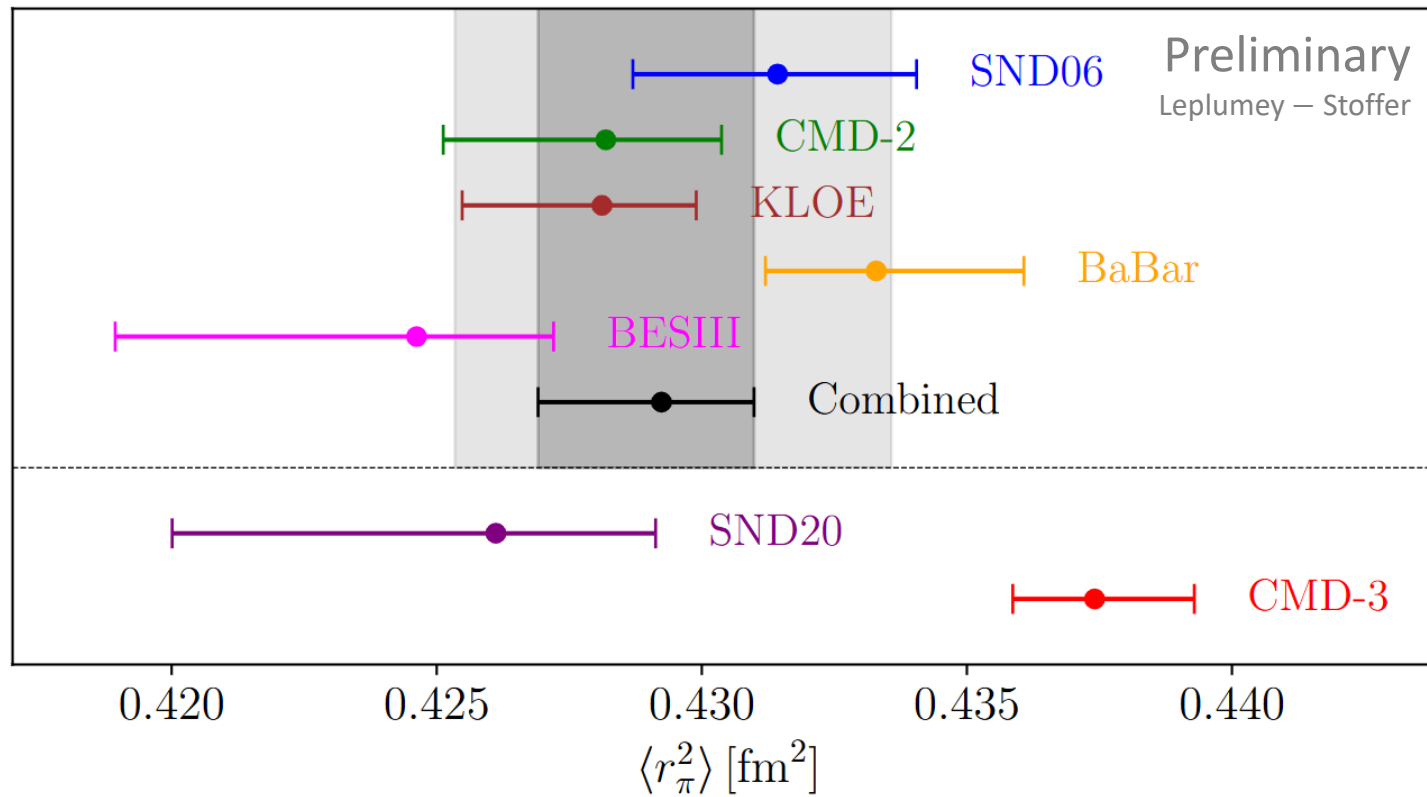
- The impact of the ω resonance is described with 3 parameters:
 - M_ω : The ω mass
 - $\text{Re}(\epsilon_\omega)$: The scale of 3π channel effects
 - $\text{Im}(\epsilon_\omega)$: The scale of $\pi^0\gamma$ channel effects

Colangelo, Hoferichter, Kubis, Stoffer, JHEP 10 (2022) 032



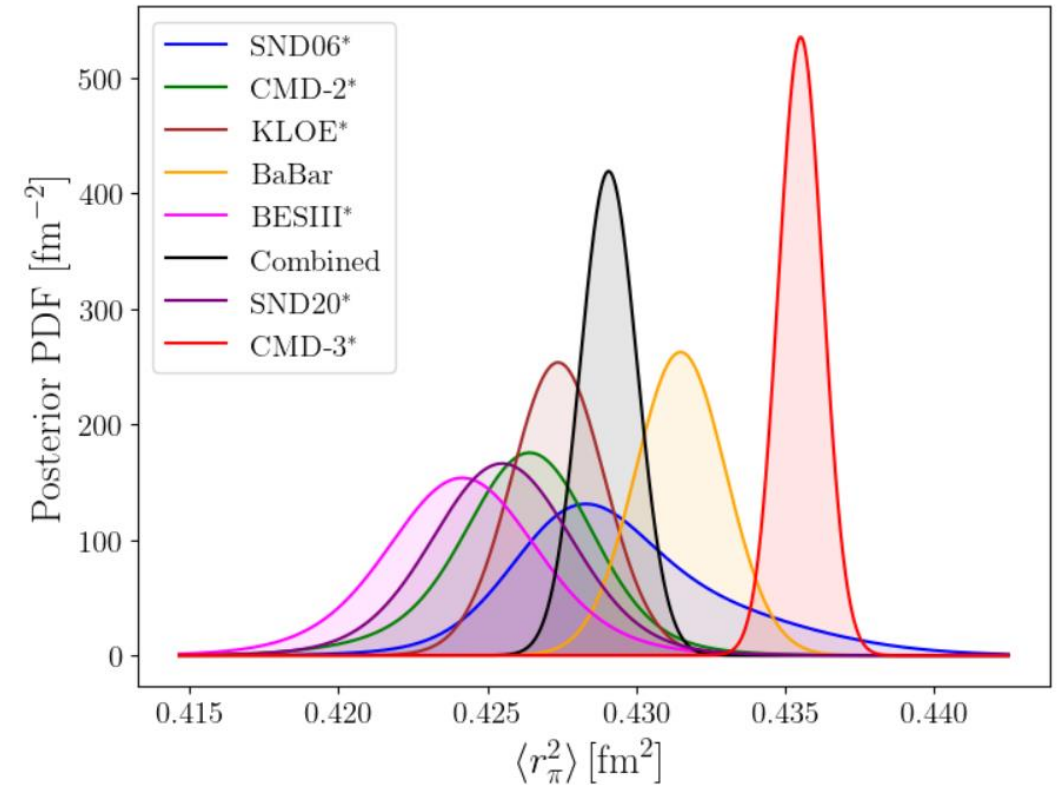
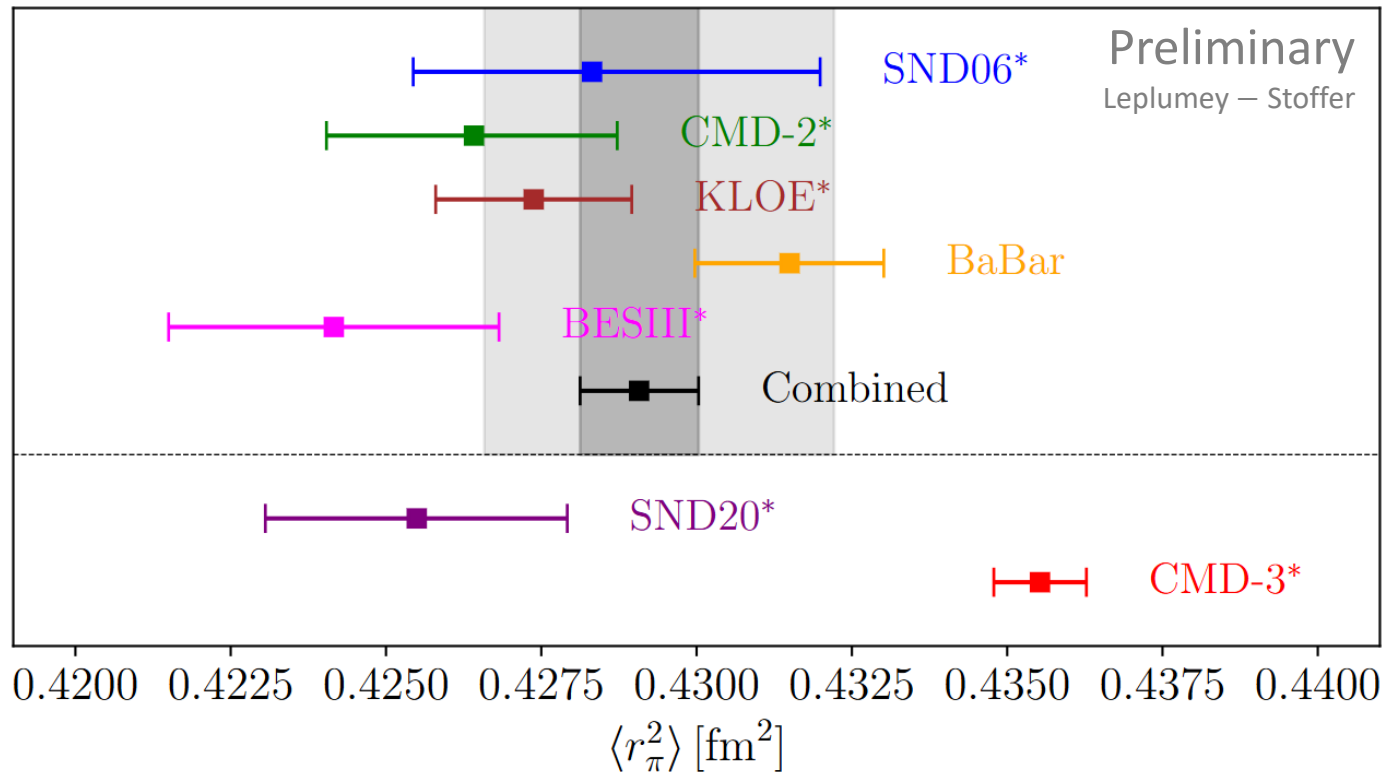
RESULT FOR THE PION CHARGE RADIUS — SUB-GeV FITS

- The impact of marginalizing on N is much more visible in the charge radius
- This appears as large non-Gaussianities in the posterior distributions



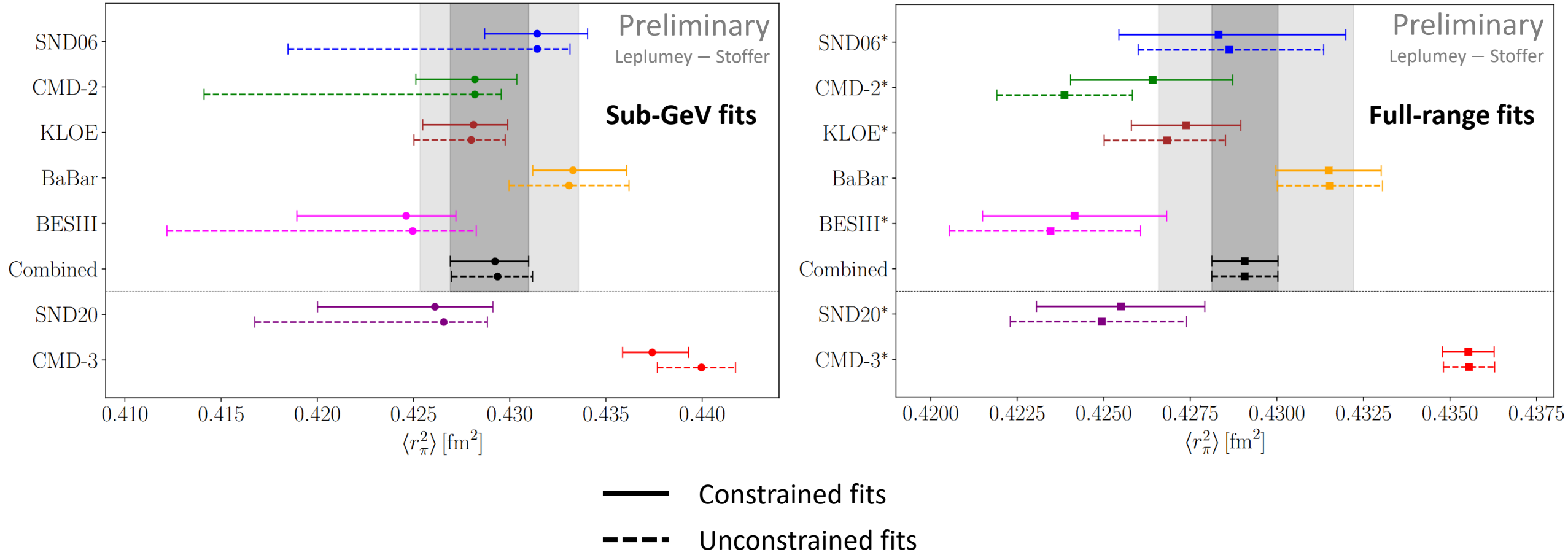
RESULT FOR THE PION CHARGE RADIUS — FULL-RANGE FITS

- However, better Gaussianity is restored in multi-GeV fits
- Multi-GeV data helps a lot in reducing the variability of the result with N



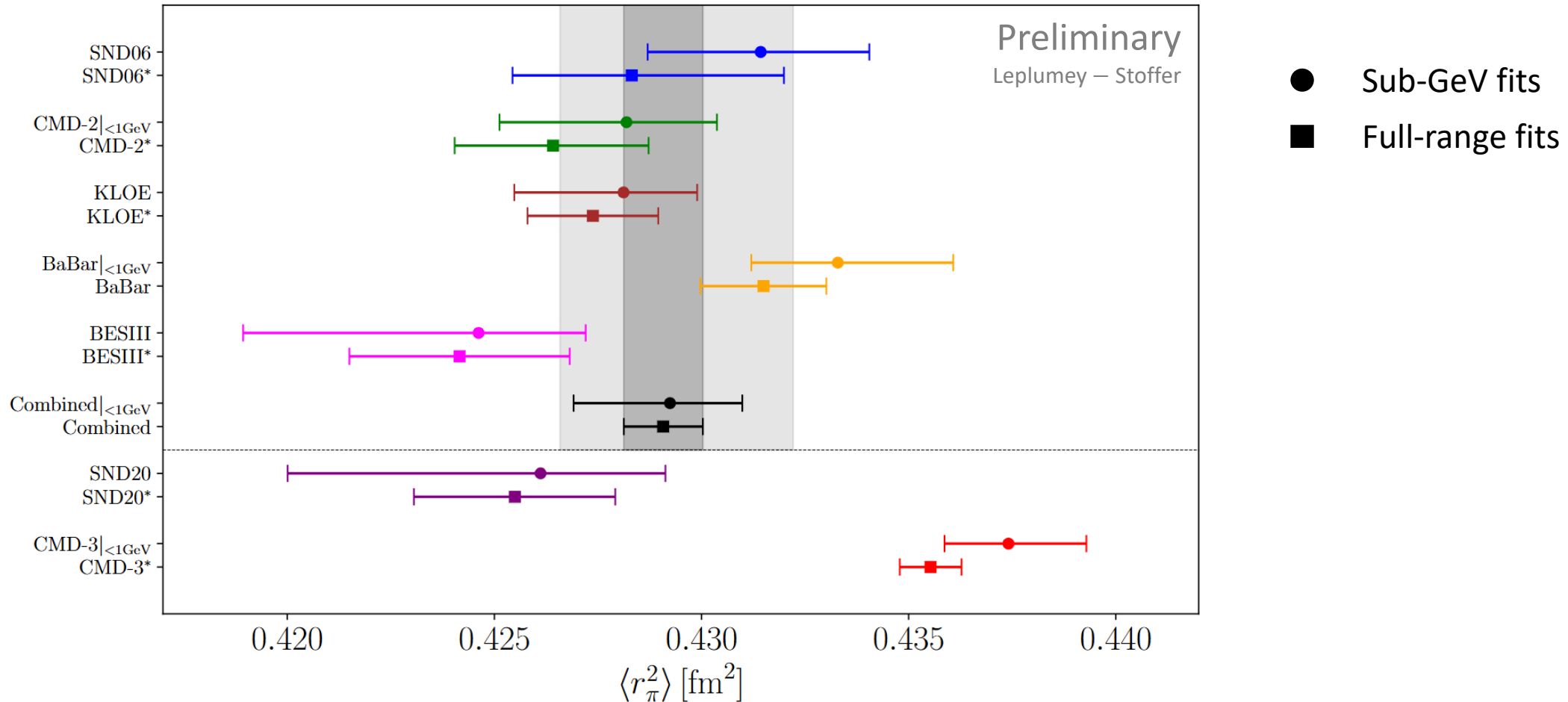
IMPACT OF ZEROS IN THE FIRST RIEMANN SHEET

- Excluding zeros reduces a lot the variability with N for sub-GeV fits
- However, the impact of zeros is almost invisible in multi-GeV fits even in $\langle r_\pi^2 \rangle$

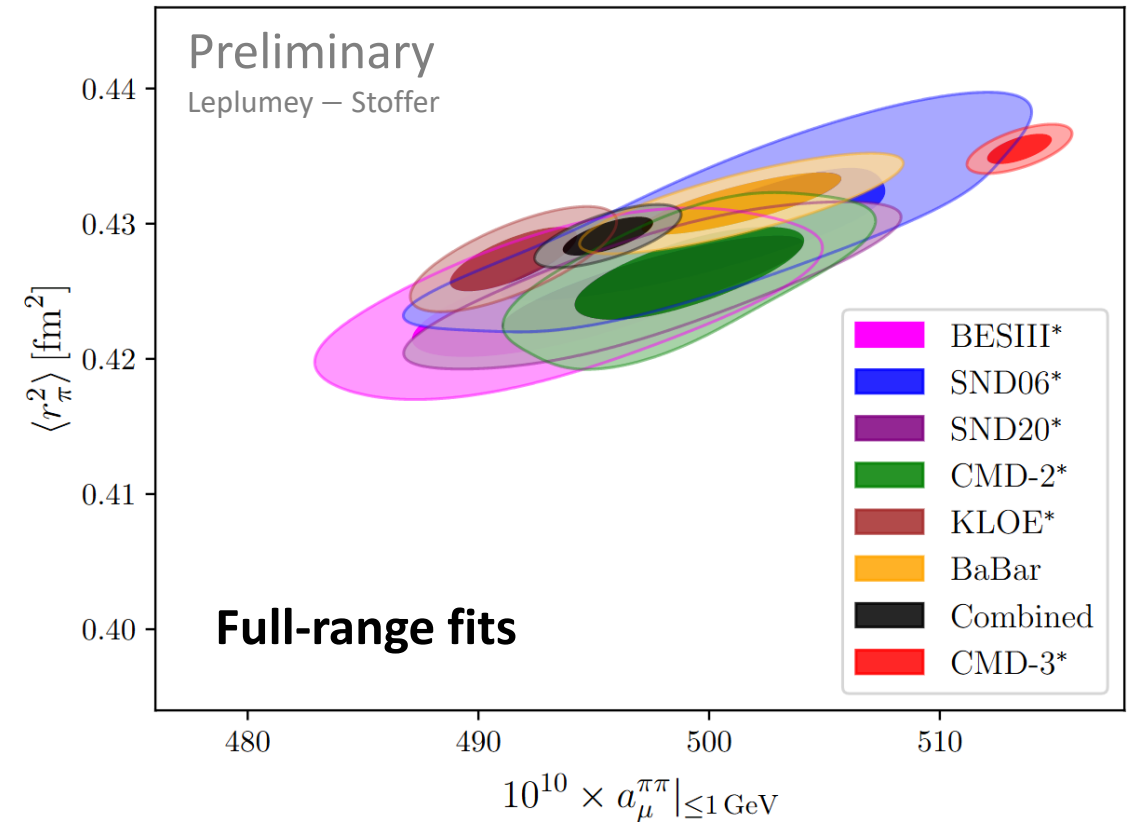
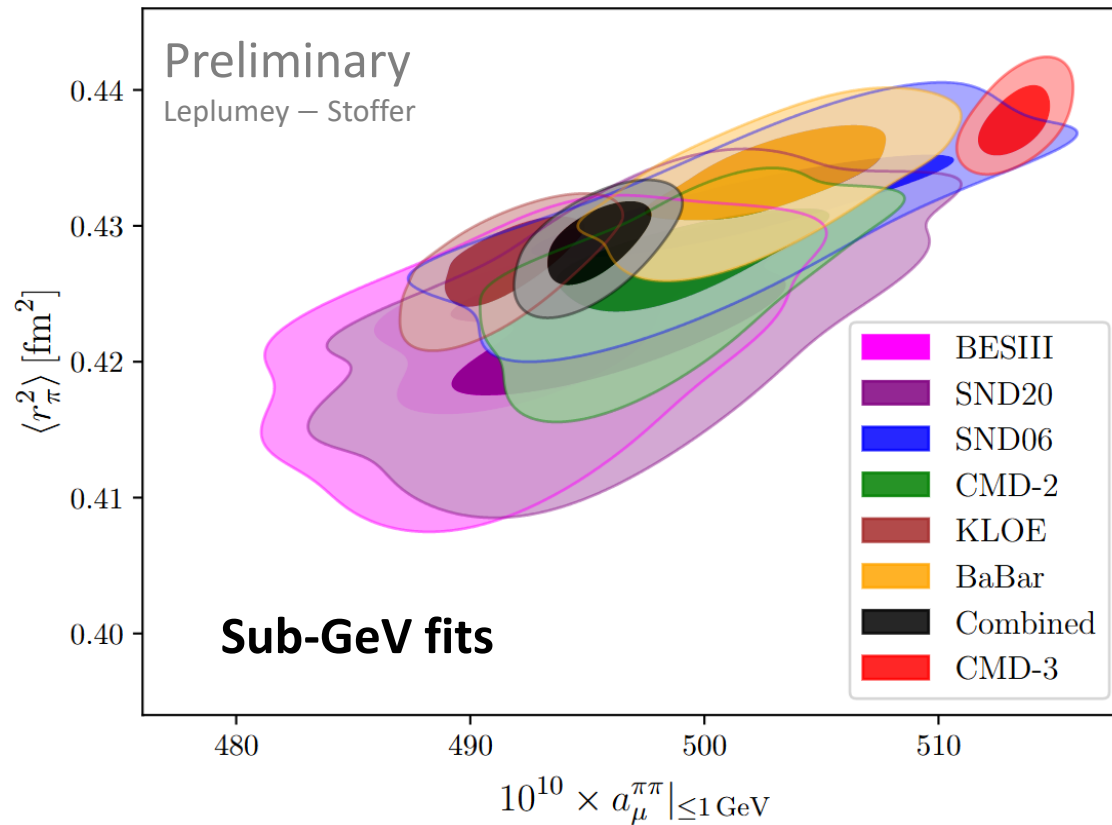


IMPACT OF MULTI-GeV DATA ON THE PION CHARGE RADIUS

- Small variations are observed (although always less than $\sim 1\sigma$)
- The inclusion of multi-GeV data systematically reduces the value of $\langle r_\pi^2 \rangle$

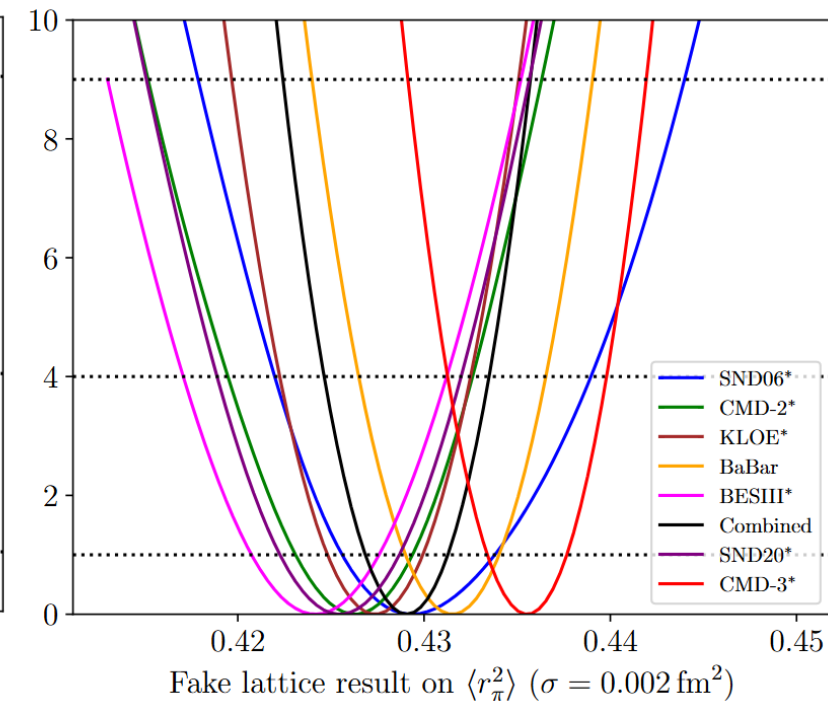
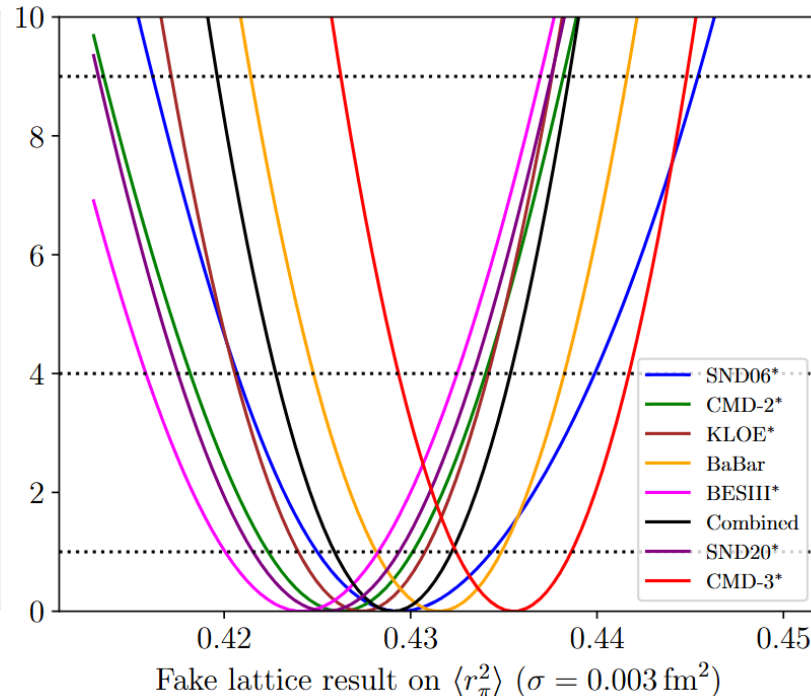
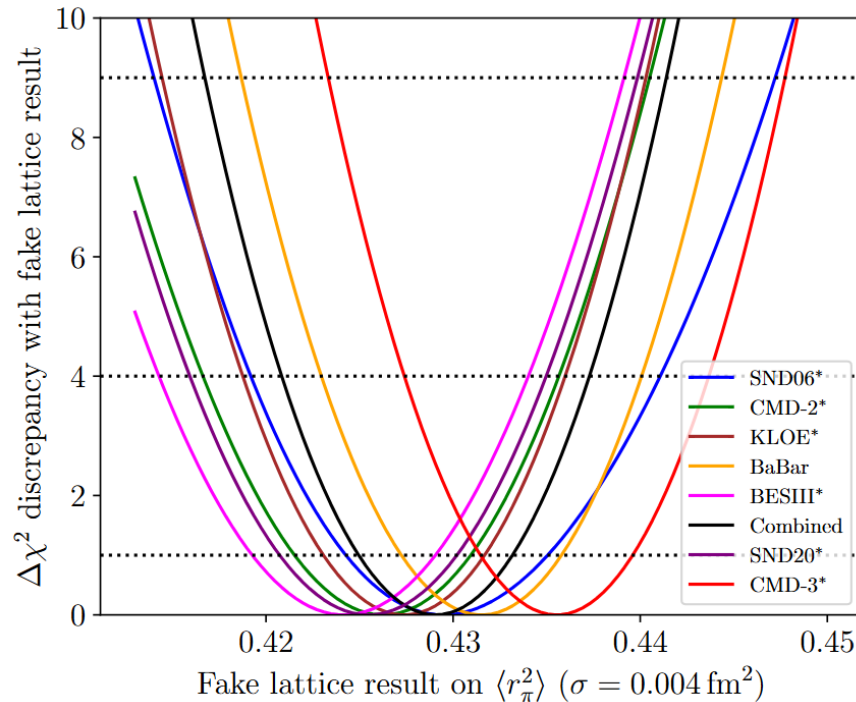


- **Strong correlations are observed between $\langle r_\pi^2 \rangle$ and $a_\mu^{\pi\pi}$** , both within each fit and between the fits
- Therefore, **an independent lattice calculation of $\langle r_\pi^2 \rangle$ could provide valuable insights on the observed discrepancies in $a_\mu^{\pi\pi}$**

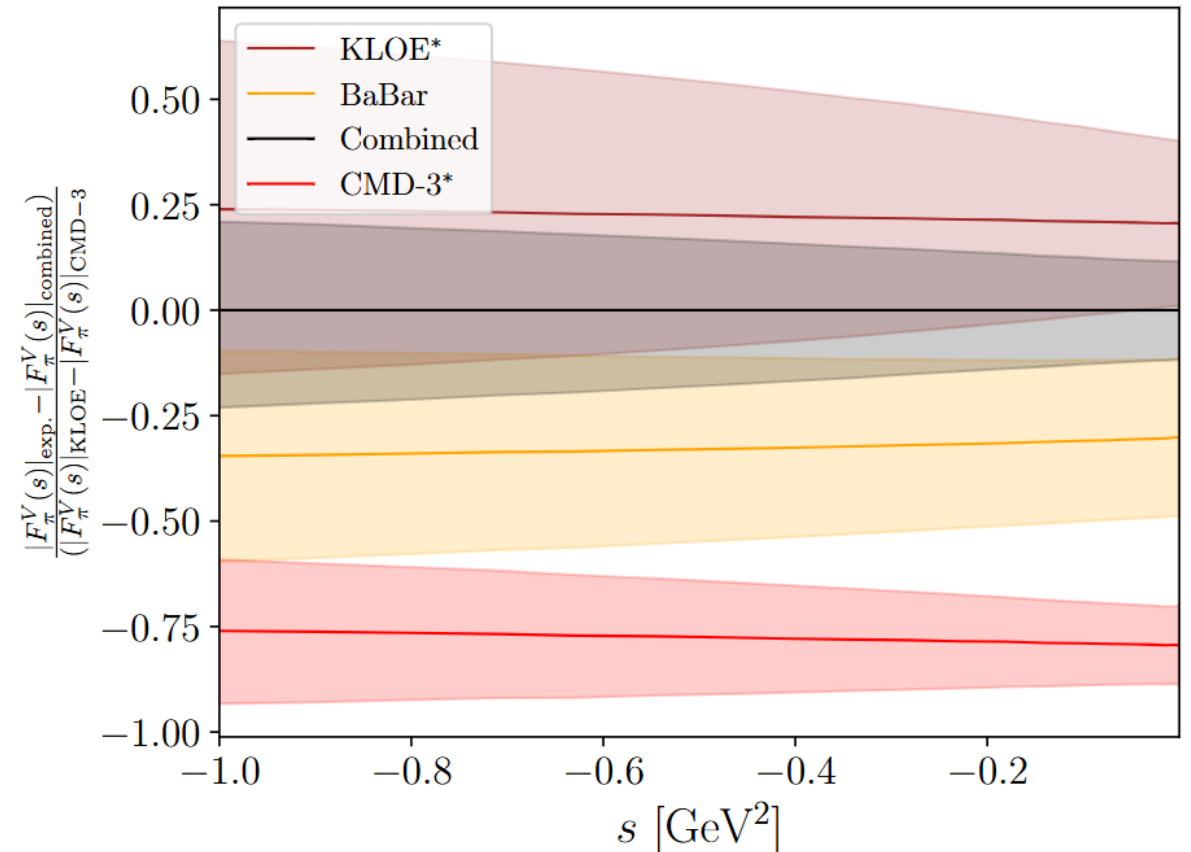
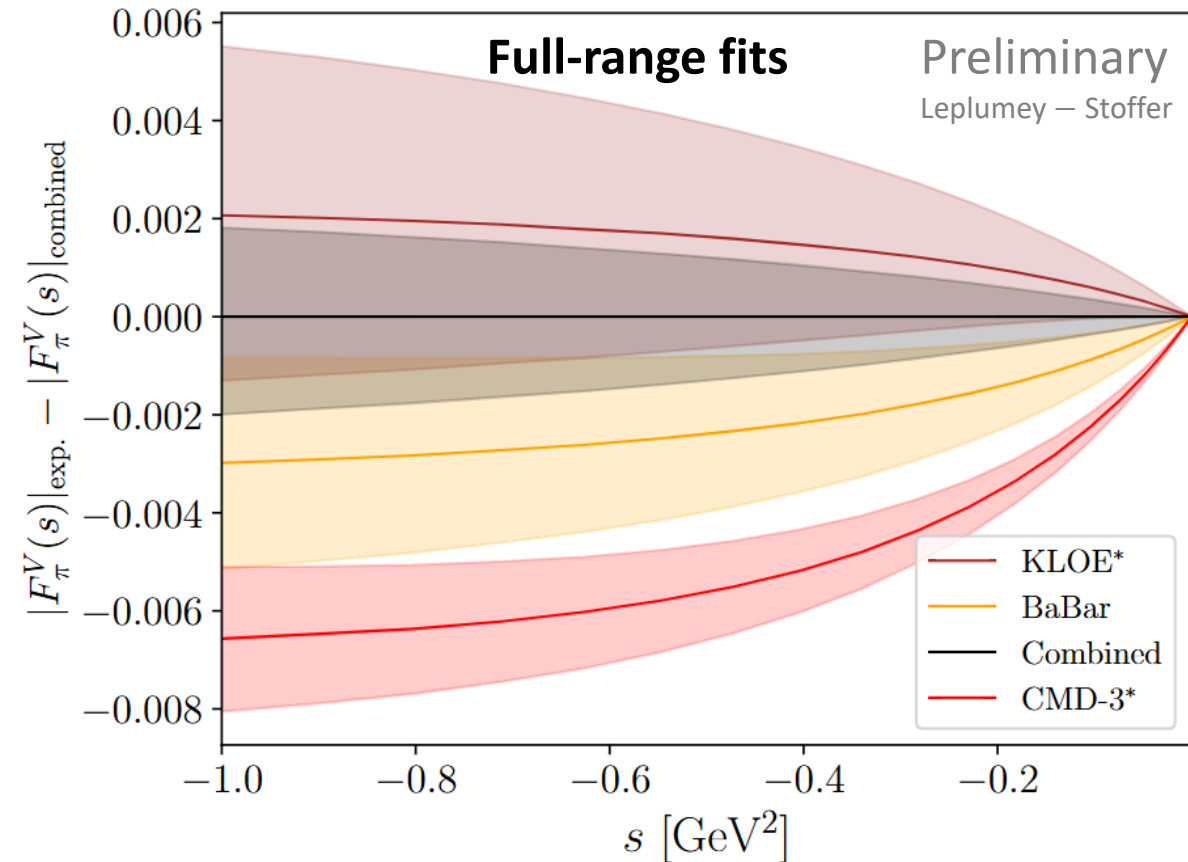


IMPACT OF A FUTURE LATTICE DETERMINATION OF $\langle r_\pi^2 \rangle$

- The impact of a **future precise lattice calculation of $\langle r_\pi^2 \rangle$** can be assessed by the expected discrepancy with current results
 - The current world-leading χ QCD result has $\sigma \sim 0.014 \text{ fm}^2$: more precision would be needed
 - A precision of 0.003 fm^2 (factor 4.6 reduction) would suffice to get $\sim 1.5\sigma$ tension with at least one experiment — up to 3σ in many cases



- An alternative probe to the charge radius could be **values of the VFF at fixed spacelike Q^2**
 - Values further from $Q^2 = 0$ are much easier to access on the lattice
 - A compromise has to be found with the increasing fit uncertainty at larger Q^2

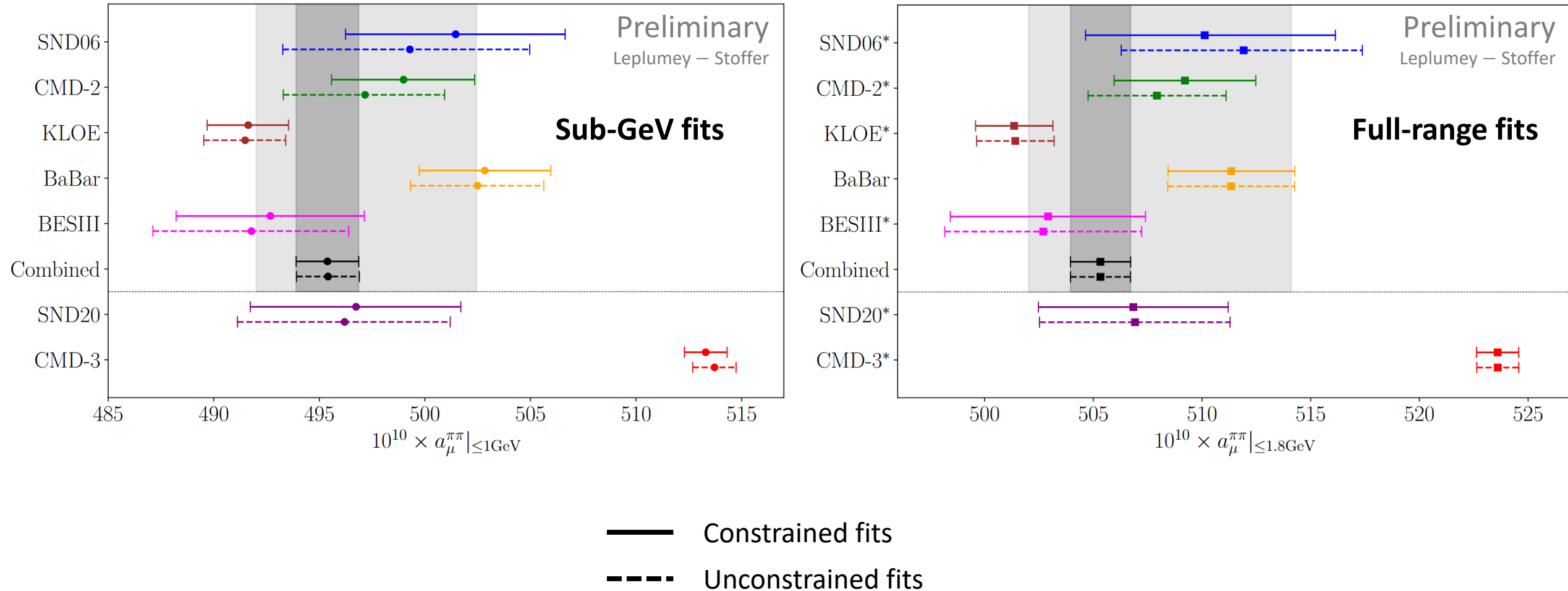


- Pion VFF representation incorporating dispersive constraints with **reduced model dependence** on full energy range
 - Determinations of $a_{\mu}^{\pi\pi}$ are **stable and robust under multiple parameterization changes**
 - Unitarity and analyticity constraints **propagate the discrepancies to the whole energy range**, including the very-long-distance window
 - The **correlations with the pion charge radius** might be very helpful to probe the discrepancies if a **precise lattice calculation of the charge radius** arises
 - Removing zeros in the physical sheet helps a lot in stabilizing the result for sub-GeV fits
 - Nevertheless, full-range fits are nearly insensitive to the constraint and naturally exclude zeros
- **Spacelike values of the VFF** might prove very valuable for **comparison with lattice calculations!**

BACKUP

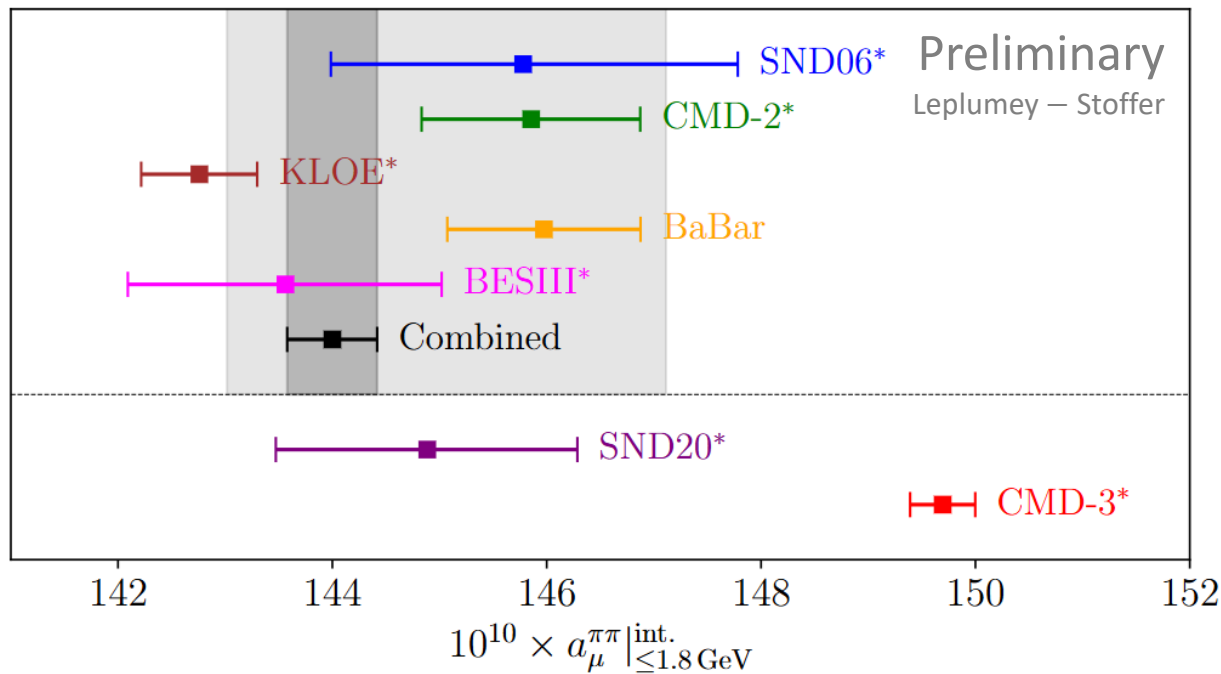
IMPACT OF ZEROS IN THE FIRST RIEMANN SHEET

- The constraint of having no zeros is almost ineffective on $a_\mu^{\pi\pi}$ alone

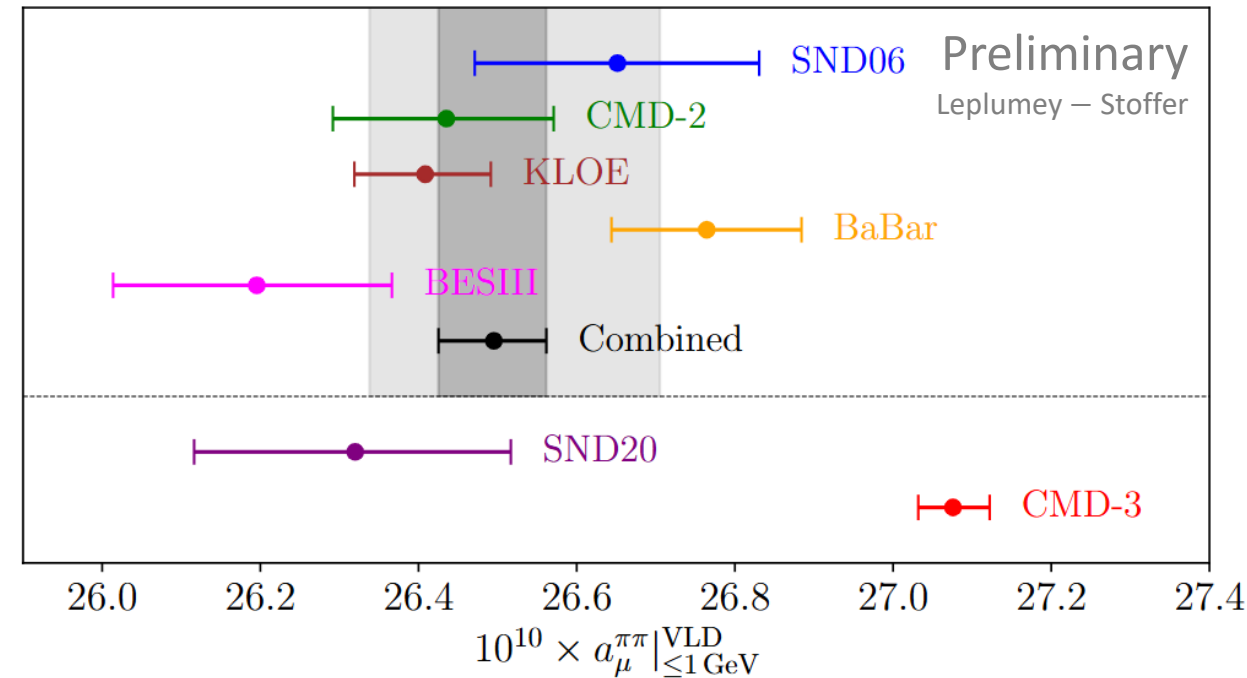


EUCLIDEAN WINDOWS

- The discrepancies are particularly visible in the intermediate window
- Still, very large discrepancies remain even at very long distance!



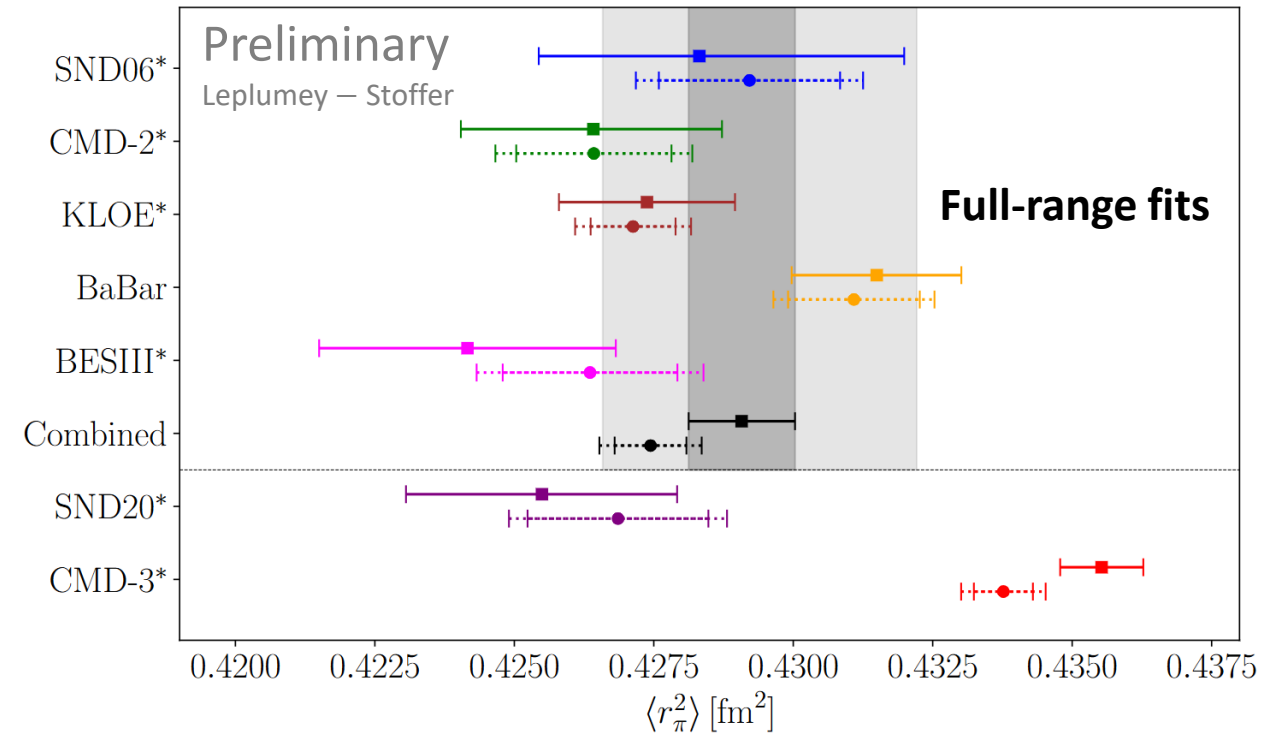
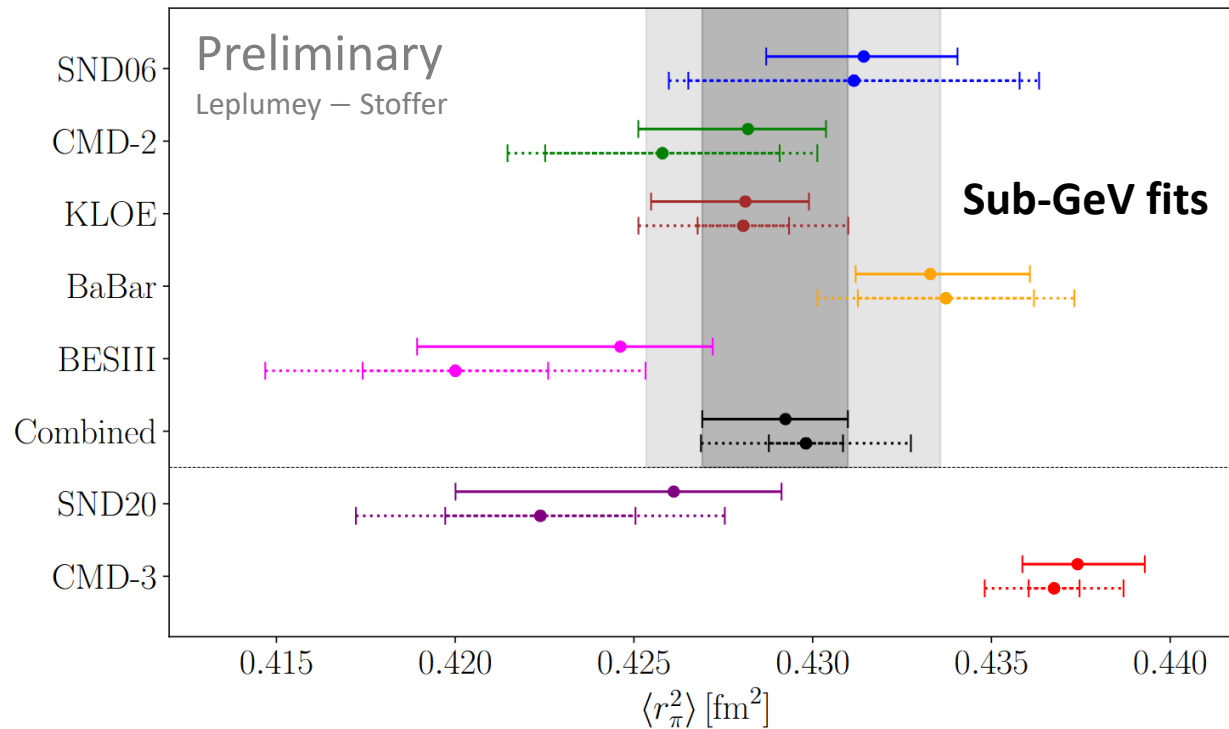
Intermediate window – full-range description



Very-long-distance window – sub-GeV description

COMPARISONS WITH OUR PREVIOUS ANALYSIS

- In sub-GeV fits, our new treatment of the systematics reduces the uncertainties
- In multi-GeV fits, switching to a less model-dependent parameterization slightly increased the uncertainties and shifted some of the results



— New analysis (preliminary)
 Previous analysis (arXiv:2501.09643)